AD-A267 322

Annual Technical Report to The Office of Naval Research and Strategic Defense Initiative Office for the Project:

Advanced Transport Systems for Electron Beams in High Brightness Accelerators and FELs"

N00014-91-J-1941

R. M. Gilgenbach, Y. Y. Lau,
T. Kammash, and M.L. Brake
Intense Energy Beam Interaction Laboratory
Nuclear Engineering Department
University of Michigan
Ann Arbor, MI 48109

for the period:
May 1, 1992-April 30, 1993

DISTRIBUTION STATEMENT A
Approved for public release;
Distribution Unlimited

DTIC
ELECTE
JUL 30 1993
S B D

93-17001
6896

93 7 28 014

REPORT DOCUMENTATION PAGE

Form Approved
OMB No. 0704-0188

Public reporting burden for this collection of information is estimated to average 1 hour per response, including the time for reviewing instructions, searching existing data sources, gathering and maintaining the data needed, and completing and reviewing the collection of information. Send comments regarding this burden estimate or any other aspect of this collection of information, including suggestions for reducing this burden, to Washington Headquarters Services, Directorate for information Operations and Reports, 1215 Jefferson Davis Highway, Suite 1204, Arlington, VA 22202-4302, and to the Office of Management and Budget, Paperwork Reduction Project (0704-0188), Washington, DC 20503.

1. AGENCY USE ONLY (Leave blank)	2. REPORT DATE	3. REPORT TYPE AND DATES COVERED
	7/19/93	Annual: 5/1/92-4/30/93

4. TITLE AND SUBTITLE
Advanced Transport Systems for Electron Beams in High Brightness Accelerators and FELS

5. FUNDING NUMBERS
ONR Contract
SFRC Number
N00014-91-J-1941

6. AUTHOR(S)
Gilgenbach, Lau, Kammash, and Brake

7. PERFORMING ORGANIZATION NAME(S) AND ADDRESS(ES)
Nuclear Engineering Department
University of Michigan
Ann Arbor, MI 48109-2104

8. PERFORMING ORGANIZATION REPORT NUMBER

9. SPONSORING/MONITORING AGENCY NAME(S) AND ADDRESS(ES)
Strategic Defense Initiative
Innovative Science and Technology/
Office of Naval Research

10. SPONSORING/MONITORING AGENCY REPORT NUMBER

11. SUPPLEMENTARY NOTES

12a. DISTRIBUTION/AVAILABILITY STATEMENT
Approved for public release;
distribution is unlimited.

12b. DISTRIBUTION CODE

13. ABSTRACT *(Maximum 200 words)*

Research on the beam breakup (BBU) instability has been performed on the following tasks during the past year:

1) Cold-test and circuit-model analysis to evaluate coupled cavity BBU experimental results,
2) Demonstration of scaling of BBU growth in a new 19 cavity system that doubles the propagation distance to about two meters,
3) Novel theoretical analysis of BBU growth in a high current annular electron beam, and
4) Theoretical studies of BBU control by gas focusing.

14. SUBJECT TERMS
Electron beams, accelerators, beam-breakup-instability

15. NUMBER OF PAGES
55

16. PRICE CODE

17. SECURITY CLASSIFICATION OF REPORT	18. SECURITY CLASSIFICATION OF THIS PAGE	19. SECURITY CLASSIFICATION OF ABSTRACT	20. LIMITATION OF ABSTRACT
UNCLASSIFIED	UNCLASSIFIED	UNCLASSIFIED	Unlimited

NSN 7540-01-280-5500

Standard Form 298 (Rev 2-89)
Prescribed by ANSI Std 239-18
298-102

Table of Contents

1.0 Summary of Research Progress

Research on the beam breakup (BBU) instability has been performed on the following tasks during the past year:

1) Cold-test and circuit-model analysis to evaluate coupled cavity BBU experimental results,

2) Demonstration of scaling of BBU growth in a new 19 cavity system that doubles the propagation distance to about two meters,

3) Novel theoretical analysis of BBU growth in a high current annular electron beam, and

4) Theoretical studies of BBU control by gas focusing.

2.0 Experimental Configuration

The experimental configuration for the 19-cavity experimnet is depicted in Figure 1. These experiments utilized the extra cavities previously used for the cavity coupling experiments enclosed in the two-meter propagation chamber. The magnetic fields obtainable from this solenoid were about a factor of two lower than the 1 meter tube, so the transported current was less. As in previous experiments, the first cavity was primed with about 1 kW of microwaves and the growth was measured between the second and last cavities. As in previous experiments, the microwave power from the second and last cavity probes was transported to the Faraday cage for comparison of the RF amplitudes.

Figure 1. Experimental Configuration

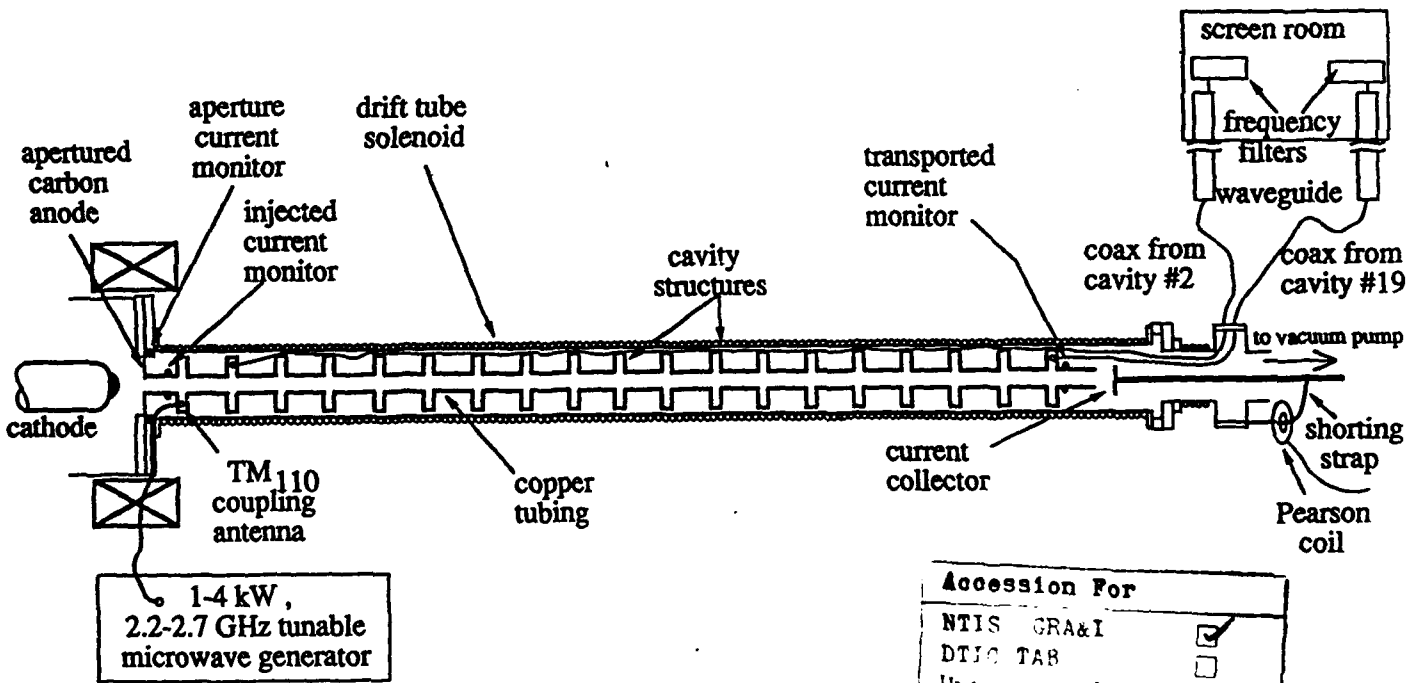

DTIC QUALITY INSPECTED 3

Accession For
NTIS GRA&I
DTIC TAB
Unannounced
Justification
By
Distribution/
Availability Codes
Dist | Avail and/or Special
A-1

3.0 Experimental Results

3.1 Nineteen Cavity BBU Experiment

In order to further test BBU scaling, we doubled the length of the propagation to two meters with 19 cavities. The results for the 19 cavity experiments are shown in figure 2, in the data points on the left hand side. It can be seen that the agreement between theory and experiments is excellent. Comparison of this data with previous 10 cavity experiments (shown on the right-hand side of the plot) shows the slope of the growth plot is nearly twice as high for the 19 cavity system, as expected.

Figure 2.

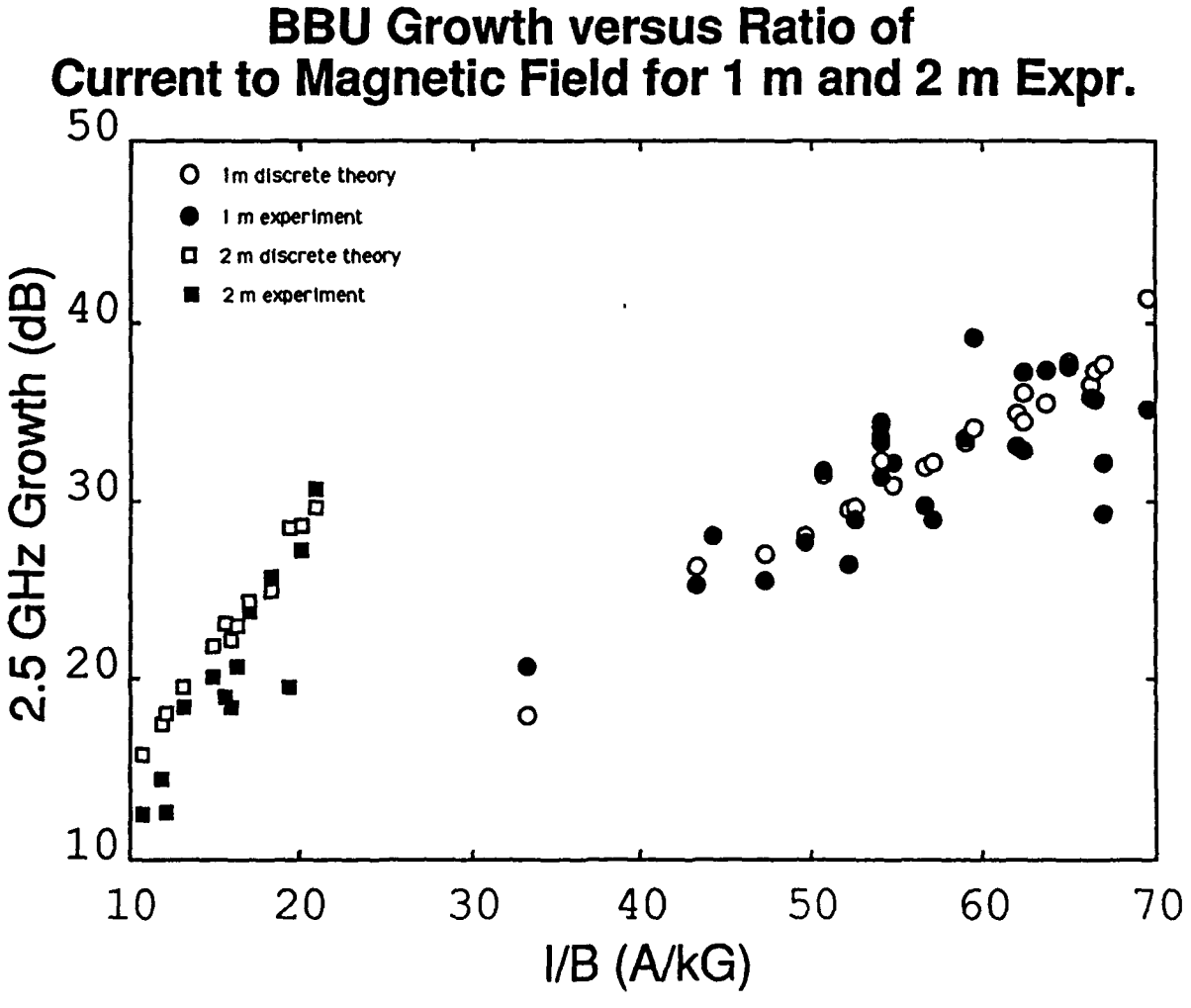

3.2 Analysis of the Cavity Coupling Experimental Data

In the original analysis of the cavity coupling experiment, we made use of a cold test which measured the ratio of power in a dummy cavity to the power in the main cavity using two model cavities which each possessed two coupling loops (Figure 3). Since the actual experiment contained cavities with one coupling loop, a correction needs to be made to account for the additional inductance of the second loop. The equivalent cold test circuit is depicted in Figure 4 and the equivalent e-beam experimental circuit is shown in Figure 5. Using this realistic equivalent circuit, the coupling κ^2Q^2 is found to be 0.18, very close to the theoretical value of 0.2 for the observed 30 dB BBU growth with coupled cavities.

Figure 3.

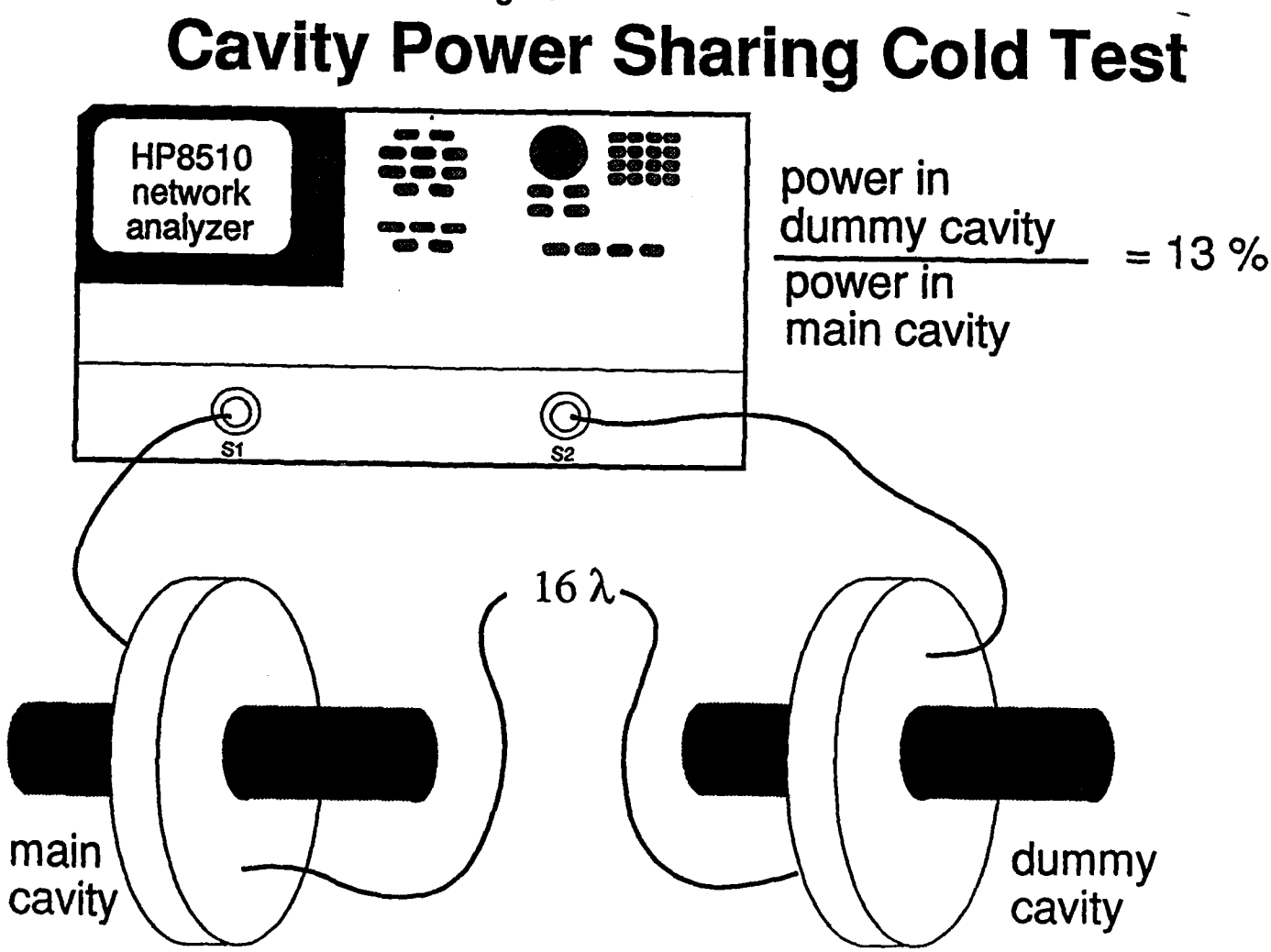

Figure 4.

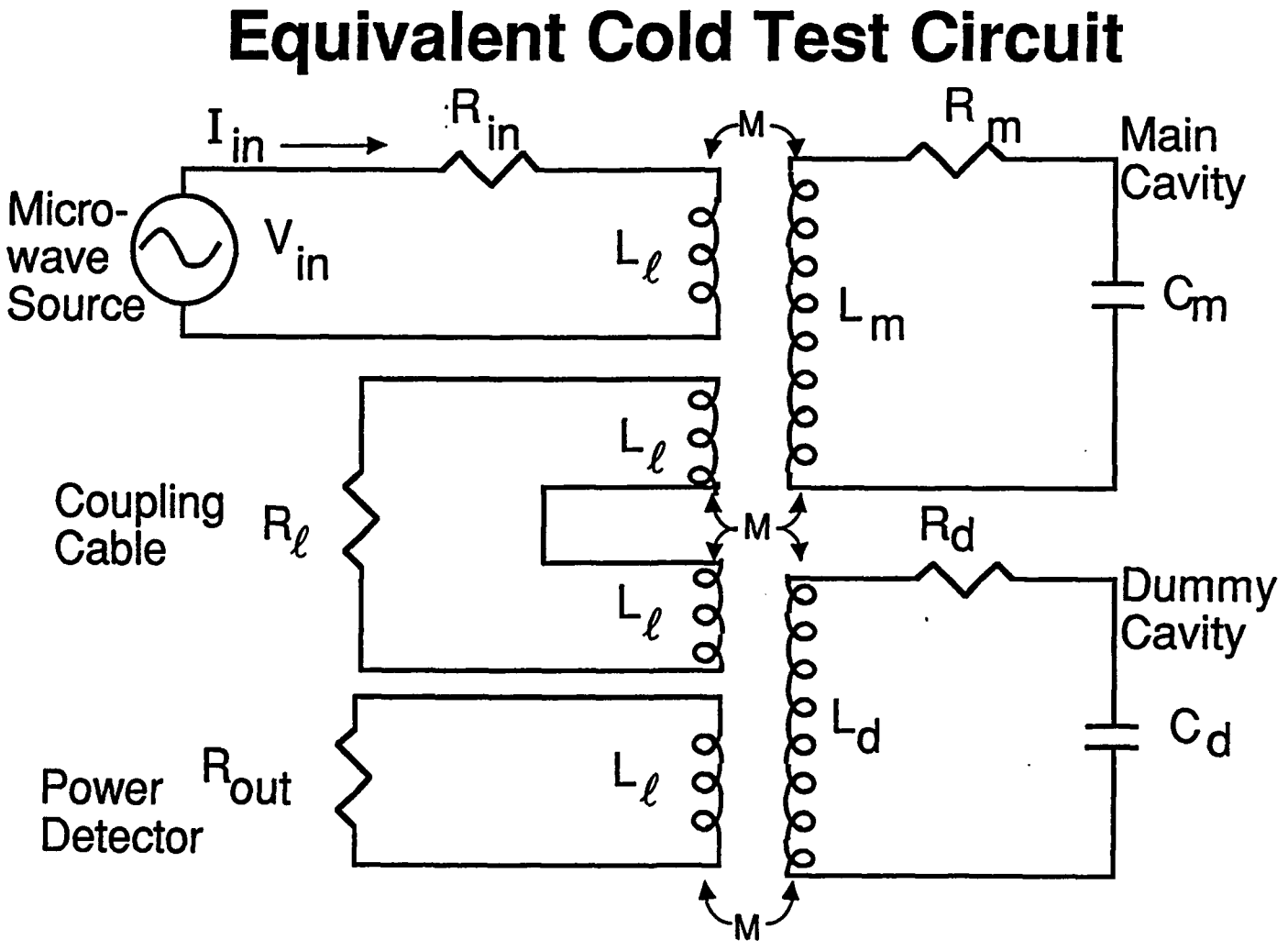
Equivalent Cold Test Circuit
I in
R in
M
R m
Main Cavity
Micro-wave Source
V in
L ℓ
L m
C m
L ℓ
Coupling Cable
R ℓ
M
R d
L ℓ
Dummy Cavity
L d
C d
Power Detector
R out
L ℓ
M

Figure 5.

Equivalent Experimental Circuit

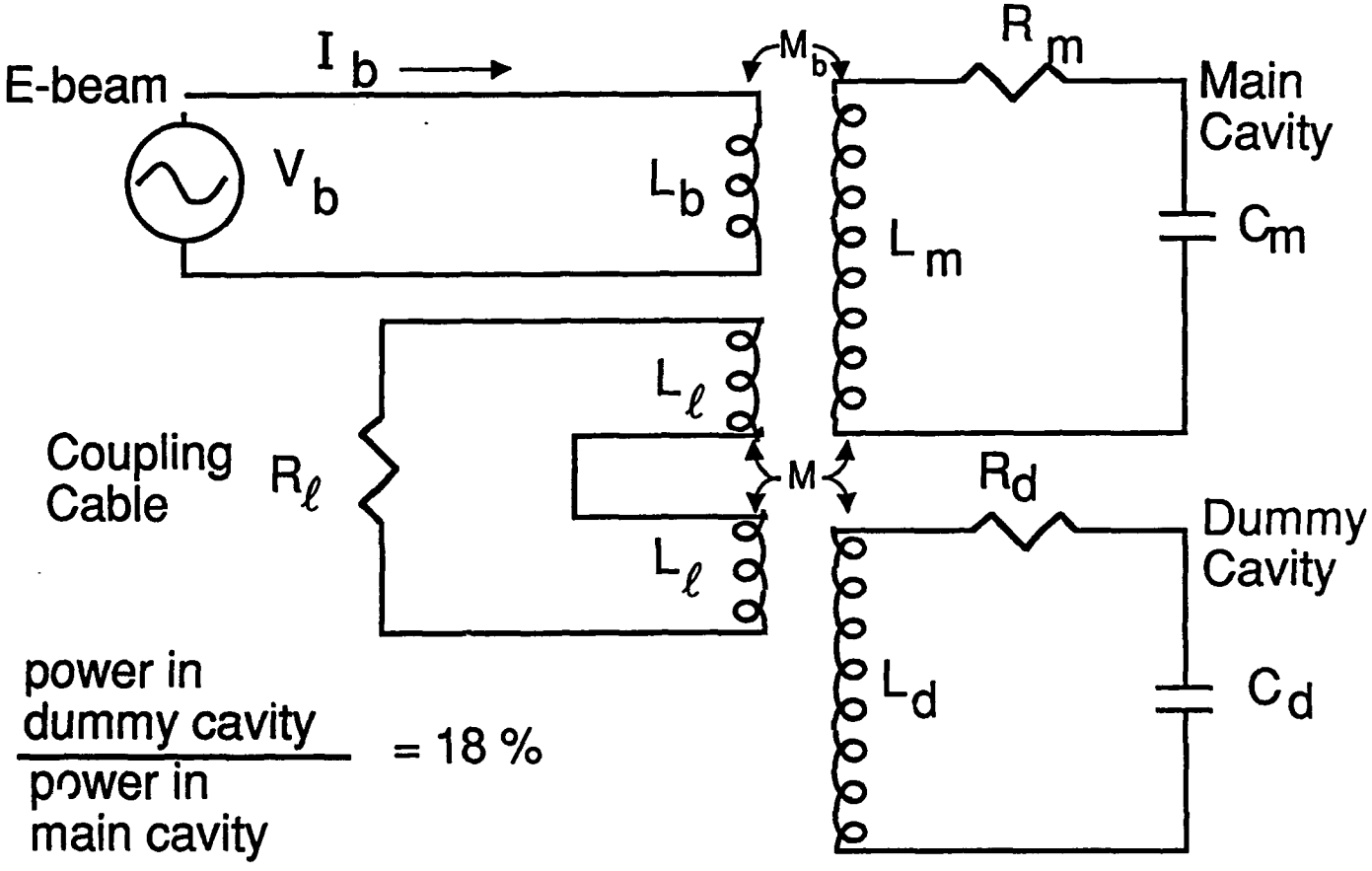

4.0 Theoretical Results

4.1 Beam Breakup in an Annular Beam

Virtually all BBU studies in the past have considered a pencil beam. In many high current devices, such as the 2-beam accelerators, annular beams are often used as a driver because of their capability in carrying a high current. This high current may then subject the beam to BBU growth.

We have carried a new theoretical study of BBU in an annular beam. We found that an annular beam may carry six (6) times as much current as a pencil beam for the same BBU growth [See Fig. 6]. The underlying reason is that the deflecting magnetic field of the dangerous mode is much weaker in the case of annular beam. This interesting finding, together with a proposed proof-of-principle experiment, is being considered for publication in J. Appl. Phys. (Rapid Communication). A copy of the preprint is attached.

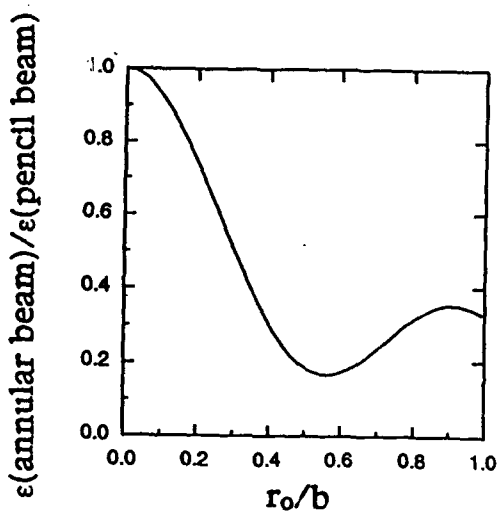

Fig. 6. Comparison of the coupling constant, epsilon, between an annular beam of radius ro and an on-axis pencil beam (ro -> 0) with the same total current. Note that when ro = 0.55 b (b = pillbox cavity radius), epsilon is a factor of 1/6 lower than that for an on-axis pencil beam.

4.2 BBU Control by Gas Focusing

Several control mechanisms have been suggested in recent years to suppress the Beam Breakup unstability (BBU). Among these are the lowering of the quality factor (Q) of the deflecting modes, linear and non-linear focusing by solenoidal magnetic fields, detuning of the cavities, and the use of pre-ionized gas channels. We focused our attention on the last approach. Since it has been for sometime that sufficiently low background gas pressure provides a medium for the transport of an intense relativistic electron beam, we singled out the beam-induced, ion focused channel as the approach that might provide sufficient focusing to suppress the BBU instability.

Using the rigid rod model for the beam, and assuming a time-dependent charge neutralization factor that varies continuously during the beam pulse, we deduced an appropriate dispersion equation which we analyzed, and compared with other mechanisms. We found that beam-induced gas focusing without cavity mode frequency spread would not fully stabilize the BBU instability. We also found that gas focusing results in smaller growth rates than solenoidal focusing up to a certain value of the magnetic field beyond which solenoidal focusing becomes significantly more effective.

5.0 Honors and Awards

R. M. Gilgenbach received the Excellence in Research Award from the University of Michigan College of Engineering in January 1993.

Mary L. Brake received the1993 Distinguished Faculty Award sponsored by the Michigan Association of Governing Boards, to recognize distinguished faculty from each of the public four year institutions in the state.

6.0 Publications and Doctoral Dissertations

Refereed Journals

1) "Experimental Reduction of Beam Breakup Instability Growth by External Cavity Coupling in Long-Pulse Electron Beam Transport", P.R. Menge, R. M. Gilgenbach, and Y. Y. Lau, Physical Review Letters, Vol. 69, page 2372, (1993)

2) "Microwave growth form the beam breakup instability in long-pulse electron beam transport", P. R. Menge, R. M. Gilgenbach, and R. A. Bosch, Applied Physics Letters, Vol. 61, p642 (1992)

3) Beam breakup in an annular beam", Y.Y. Lau and J. Luginsland, submitted to J. Appl. Phys. (Rapid Communication).

4) "Beam breakup growth and reduction experiments in long-pulse electron beam transport", P. R. Menge, R. M. Gilgenbach, Y. Y. Lau, and R. A. Bosch, in preparation for Journal of Applied Physics

Conference Papers

1) Beam breakup in an annular beam", Y.Y. Lau, J. Luginsland, and R. M. Gilgenbach, Presented at 1993 Particle Accelerator Conference, May 1993, Washington, D.C.

2) "Experimental Reduction of electron beam breakup instability using external coupled cavities", P. R. Menge, R. M. Gilgenbach, Y.Y. Lau, M. Walter,

and C.H. Ching, Presented at 1993 Particle Accelerator Conference, May 1993, Washington, D.C.

3) "Electron Beam-breakup-instability growth reduction experiments using external coupled-cavities", P. R. Menge, R. M. Gilgenbach,, M. Walter, C.H. Ching and Y.Y. Lau, Presented at the 1992 Annual Meeting of the Division of Plasma Physics of the APS.

Doctoral Dissertation

1) P. R. Menge, "Experimental excitation and reduction of the beam breakup instability in long-pulse electron beam transport, defended in April 1993

7.0 Personnel Involved in This Research

1) R. M. Gilgenbach
2) Y. Y. Lau
3) Mary L. Brake
4) T. Kammash
5) P. R. Menge
6) J. Luginsland
7) D. Galbraith

Experimental Reduction of Beam-Breakup Instability Growth by External Cavity Coupling in Long-Pulse Electron-Beam Transport

P. R. Menge, R. M. Gilgenbach, and Y. Y. Lau

Intense Energy Beam Interaction Laboratory, Nuclear Engineering Department, University of Michigan, Ann Arbor, Michigan 48109-2104

(Received 24 July 1992)

Experiments have demonstrated the reduction of the beam-breakup (BBU) instability growth rate by coupling the main cavities, through which an electron beam passes, to identical dummy cavities. When seven of the ten main cavities are coupled, an average reduction of about 6 dB in BBU microwave growth, from 36 to 30 dB, is observed. This reduction is consistent with a simple mode coupling theory. The electron beam parameters are 750 kV, 210 A, 0.5 μs, with solenoidal focusing of 3.4 kG.

PACS numbers: 41.75.Ht, 41.85.Ja, 52.70.Gw

Beam breakup (BBU) [1–7] is a major instability that limits the current and pulse length of linear accelerators. Several methods have been found to reduce such instability growth, including stagger tuning [2,7–9] of the cavity resonant frequencies and cavity loading in which the dominant deflecting mode is heavily damped by slots [10] or by ferrite [11]. Betatron frequency spreads have also been shown to lower BBU growth [8,12–14].

It has been recently predicted [15] that, by simply coupling the accelerating (main) cavities to identical dummy cavities, BBU growth may be reduced. This reduction occurs, according to the conjecture given in Ref. [15], because the dummy cavities share the power of the deflecting mode excited by the beam, thereby lowering the deflecting mode amplitude in the main cavities that drives the electron beam unstable. It should be emphasized that BBU control by coupled cavities is purely reactive instead of dissipative, the latter having been extensively pursued with the use of lossy materials or slots. This paper reports our experimental investigation of this concept, using a long-pulse (0.5–1 μs) electron beam of extracted current 40–400 A, guided by a solenoidal magnetic field of 1–4 kG. These parameters span the intermediate regime, where the effect of focusing field is marginally important.

The experiment is driven by the Michigan Electron Long-Beam Accelerator (MELBA) [16], which operates with diode parameters of voltage $=-0.7$ to -0.8 MV, diode current $=1$–15 kA, and flattop pulse length of 0.5–1 μs. The experimental configuration is shown in Fig. 1. The electron beam is produced by a velvet button cathode on the hemispherical end of the cathode stalk. A graphite aperture defines the 2-cm injected beam diameter and yields extracted currents of 40–400 A. The

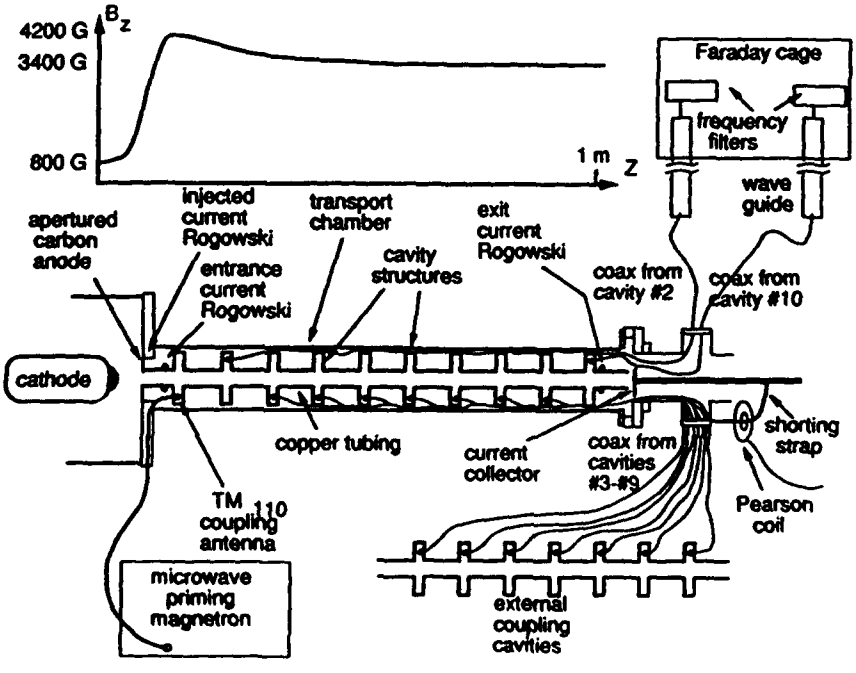

FIG. 1. Schematic of experimental configuration (lower) and magnetic field profile (upper).

© 1992 The American Physical Society

anode cathode gap is about 10.2 cm. The diode chamber is immersed in a uniform solenoidal magnetic field that can be varied from 0.5 to 1.2 kG. The beam transport chamber is a stainless-steel tube wound with pulsed solenoidal magnetic field coils. These coils produce a magnetic field that can range from 1 to 4 kG.

Within the transport chamber are ten brass pillbox resonant cavities with a radius of 6.9 cm and a length of 2.0 cm. Separating each cavity is a smaller-radius (1.9 cm) copper tube of length 6.5 cm used to prevent electromagnetic cross talk (−26 dB measured) and thus eliminate the regenerative BBU instability. Inside each cavity is a small loop antenna (0.7 cm diameter) oriented to be sensitive to the TM_{110} mode for cold-testing and e-beam experiments. The average cold-test TM_{110} resonant frequency is 2.5075 ± 0.0026 GHz. A small annulus of microwave absorber is loaded into the cavities to lower the deflecting mode quality factor Q to an average of 215 ± 45.

The coupling loop in the first cavity is utilized for priming the TM_{110} mode with the signal from a kW-level microwave pulse generator. The priming microwave pulse is generally 3 μs long, and begins before the e beam is present. The coupling loops in the second and tenth cavities are used to measure the growth of the microwaves corresponding to the frequency of the TM_{110} beam-breakup mode [17]. The microwave signals are propagated out of the transport chamber by coaxial cables and transmitted to a Faraday cage by S-band waveguides. At the waveguide termination the microwaves are sent into a filter which passes 2.5075 ± 0.0115 GHz, thus ensuring that any measured growth is due to only the BBU signal of the TM_{110} mode resonant frequency. The microwave signals are then attenuated to a level appropriate for measurement on crystal detectors. For the coupled-cavity experiments, the coupling loops on the internal, intervening seven cavities (3 through 9) are connected to seven identical external dummy cavities by a set of equal-length (16λ) coaxial cables. For baseline experiments the cables are disconnected between the internal (main) and the seven external (dummy) cavities.

The beam current is measured in five places along the beam path. A B-dot loop in the MELBA oil tank measures the cathode stalk current. Calibrated Rogowski coils are used to determine the current injected into the transport chamber immediately after the apertured anode, just before entering the first cavity, and just after exiting the last cavity. After exiting the cavity structure, the beam propagation is terminated by a carbon collector plate grounded by a cable which passes through a Pearson current transformer.

Typical experimental data are presented in Figs. 2 and 3. In order to compare the BBU growth for the uncoupled-cavity baseline case to the coupled-cavity case, a typical experimental run alternated between three shots for each case. Figure 2 shows data signals from an uncoupled-cavity shot, while Fig. 3 presents corresponding signals from the consecutive shot in which seven pairs of cavities were coupled. The uppermost trace (a) is the MELBA diode voltage in which the flattop occurs at 750 kV and lasts for 500 ns. The second trace (b) shows the microwave power in the second cavity after passing through a frequency filter. The third trace (c) shows the microwave power in the tenth cavity after passing

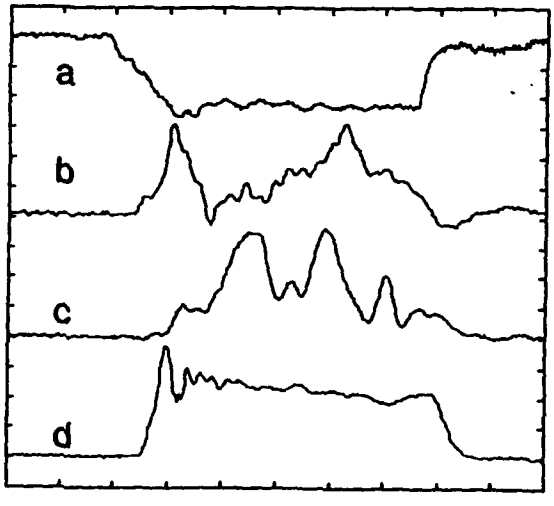

FIG. 2. Experimental data for uncoupled cavities: (a) Electron beam voltage (310 kV/div); (b) microwave diode detector signal in the second cavity, filtered at 2.5075 ± 0.0115 GHz (50 mV/div); (c) microwave diode detector signal in the tenth cavity filtered at 2.5075 ± 0.0115 GHz with 36-dB attenuation (50 mV/div); (d) transported current leaving tenth cavity (92 A/div) from a different shot. Applied solenoid field is 3.4 kG.

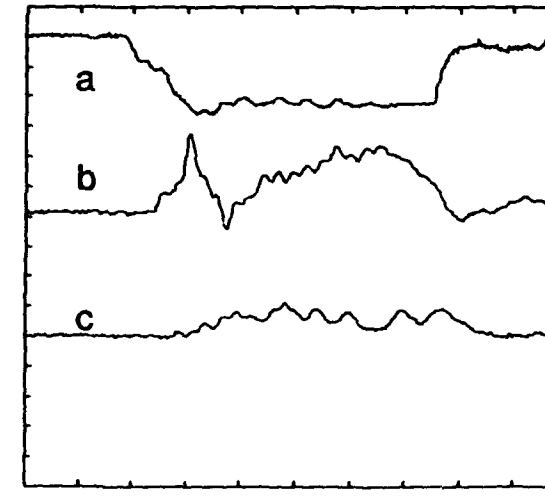

FIG. 3. Experimental data for externally coupled cavities: (a) Electron beam voltage (310 kV/div); (b) microwave diode detector signal in the second cavity, filtered at 2.5075 ± 0.0115 GHz (50 mV/div); (c) microwave diode detector signal in the tenth cavity filtered at 2.5075 ± 0.0115 GHz with 36-dB attenuation (50 mV/div). Applied solenoid field is 3.4 kG.

A-2

through a frequency filter; the microwaves have been attenuated by 36 dB. Note the approximately 4 times reduction in rf power in the tenth cavity between Figs. 2(c) and 3(c). The last trace, Fig. 2(d) is a typical transported current signal with a flattop corresponding to 210 A.

A summary of beam-breakup-instability microwave growth data from some forty shots is presented in Fig. 4(a). The data show a consistent reduction of BBU growth from an average of 36 dB ($\sigma = \pm 1.5$ dB) for the uncoupled case to an average of 30 dB ($\sigma = \pm 2.4$ dB) for the coupled-cavity case. Therefore, we measure an average BBU growth reduction of about 6 dB for the present system in which seven main cavities are coupled to dummy cavities. The variations in experimental BBU signal growth amplitudes could be related to pulse-to-pulse variations in e-beam current amplitudes, shown in Fig. 4(b). All shots were taken with a solenoidal magnetic field of 3.4 kG. The B-field profile is shown in Fig. 1.

Theoretical research on coupled cavities [15] has predicted a growth rate reduction by up to a factor of 2, depending upon the coupling strength κ between the main cavity and the dummy cavity. A simple theory of the BBU instability including coupled cavities may be developed by starting with the force law in the continuum description [1,4–7]:

$$-\gamma[(\omega - kv)^2 - \omega_\beta^2]\xi = A\,, \tag{1}$$

where A denotes the complex amplitude of the deflecting mode in the main cavity, ξ is the transverse deflection of the beam, k is the wave number, v is the e-beam velocity, γ is the usual relativistic mass factor, ω is the angular frequency of the injected signal which undergoes BBU growth, and ω_β is the relativistic betatron frequency. The main cavity is excited by the beam's transverse displacement ξ and by the dummy cavity when coupling is present. Using a simple mutual inductance model for cavity coupling, A is governed by [15]

$$LA = 2\gamma\omega_0^4\varepsilon\xi + \kappa\omega_0^2 D\,, \tag{2}$$

where D denotes the complex amplitude of the dummy cavity field, ε is the dimensionless parameter that measures BBU strength [18], ω_0 is the TM_{110} mode angular resonant frequency, and $L \equiv d^2/dt^2 + (\omega_0/Q)d/dt + \omega_0^2$ is the familiar operator. In this model, the equation for D reads

$$LD = \kappa\omega_0^2 A\,. \tag{3}$$

Equations (1)–(3) constitute three equations in three unknowns, A, D, and ξ. The BBU dispersion relation may be obtained which yields the spatial exponentiation rate k_I as a function of ω. At resonance, $\omega = \omega_0$, and for sufficiently large ω_β, it reads

$$k_I = \left(\frac{\omega_0}{v}\right) Q\varepsilon \frac{\omega_0}{\omega_\beta} \frac{1}{(1+\kappa^2 Q^2)}\,, \tag{4}$$

which shows that the BBU growth rate is reduced by a factor $1+\kappa^2Q^2$ when cavity coupling is present ($\kappa \neq 0$).

This reduction has a simple interpretation. First note that at resonance ($\omega = \omega_0$), $L = j\omega_0^2/Q$, and Eq. (3) gives

$$\kappa^2 Q^2 = \left|\frac{D}{A}\right|^2 = \frac{\text{power leaked to dummy cavity}}{\text{power in main cavity}}\,. \tag{5}$$

Thus, the factor $1/(1+\kappa^2Q^2)$ in Eq. (4) becomes the fraction of rf power that resides in the main cavity in a coupled-cavity system. In other words, the BBU growth reduction, according to Eq. (4), is a result of the sharing of rf power by the dummy cavity [19].

Experimental measurements were made of the power sharing by a pair of model cavities each having two coupling loops. The signal from an HP-8510 network analyzer was fed into one cavity which was coupled by type .405/U cable to the second cavity. The received power in the second cavity was found to correspond to 13% of the first cavity's power, or $\kappa^2Q^2 = 0.13$ according to Eq. (5). Thus, for an uncoupled BBU growth of 36

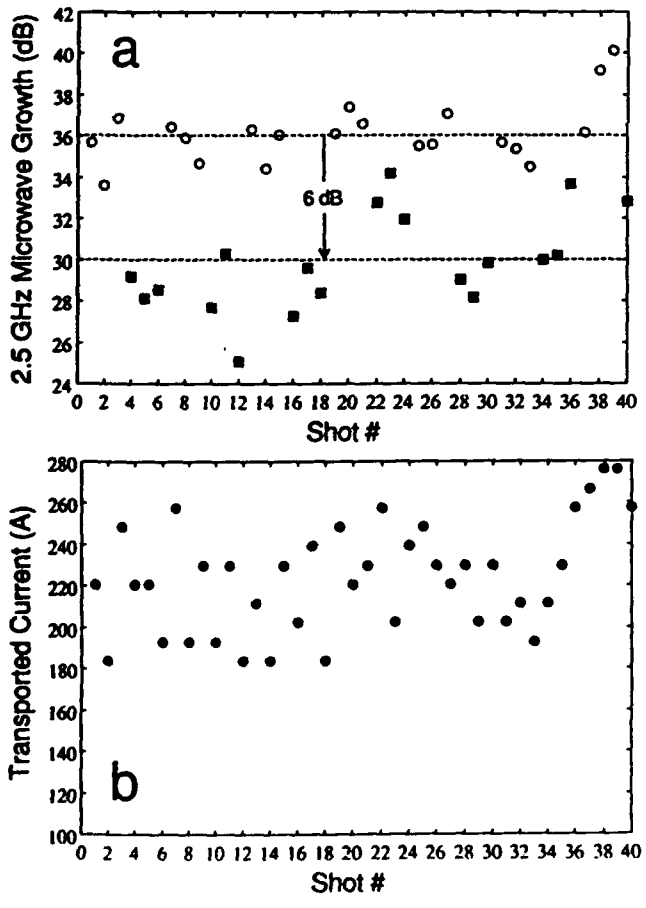

FIG. 4. (a) Growth (dB) of the 2.5-GHz microwave power for forty different electron beam pulses showing uncoupled shots (open circles) and externally coupled shots (solid squares). (b) Transported electron beam current (A) for the corresponding shot numbers of (a).

A-3

dB, the theory predicts a coupled-cavity BBU growth of 31.9 dB, consistent with the data given in Fig. 4(a). The inferred value of κ is 0.17%.

In conclusion, the coupling of seven pairs of cavities gave an experimental reduction of the beam-breakup-instability in general agreement with a very simple theoretical model. While we have made no attempt to optimize the degree of cavity coupling, it is interesting to note that a value of κ as low as 0.17% already leads to appreciable BBU reduction in a seven-cavity system, as observed in the present experiment. One may wonder if this technique of coupled-cavity beam-breakup-instability reduction would also have the tendency to control higher-order BBU modes.

We appreciate experimental assistance from M. T. Walter, C. H. Ching, and R. A. Lindley. This research was supported by SDIO-IST through an ONR contract. Part of this research was performed when one of us (Y.Y.L.) was with the Naval Research Laboratory.

[1] W. H. K. Panofsky and M. Bander, Rev. Sci. Instrum. 39, 206 (1968).

[2] R. H. Helm and G. A. Loew, in *Linear Accelerators*, edited by R. P. Lapostolle and A. L. Septier (North-Holland, Amsterdam, 1970), p. 173.

[3] K. Neil, L. S. Hall, and R. K. Cooper, Part. Accel. 9, 213 (1979); 1, 111 (1979).

[4] Y. Y. Lau, Phys. Rev. Lett. 63, 1141 (1989).

[5] R. A. Bosch, P. R. Menge, and R. M. Gilgenbach, J. Appl. Phys. 71, 3091 (1992).

[6] A. W. Chao, B. Richter, and C. Y. Yao, Nucl. Instrum. Methods 178, 1 (1980).

[7] C. L. Bohn and J. R. Delayen, Phys. Rev. A 45, 5964 (1992).

[8] D. G. Colombant and Y. Y. Lau, Appl. Phys. Lett. 55, 27 (1989); 53, 2602 (1988).

[9] R. L. Gluckstern, F. Neri, and R. K. Cooper, Part. Accel. 23, 37 (1988).

[10] F. Voelker, G. Lambertson, and R. Rimmer, in *1991 IEEE Particle Accelerator Conference* [IEEE Catalog No. 91 CH3038-7, 2, 687 (1991)].

[11] G. J. Caporaso, A. G. Cole, and K. W. Struve, IEEE Trans. Nucl. Sci. 30, 2507 (1983).

[12] G. J. Caporaso, F. Rainer, W. E. Martin, D. S. Prono, and A. G. Cole, Phys. Rev. Lett. 54, 685 (1985).

[13] D. Chernin and A. Modelli, Part. Accel. 24, 177 (1989).

[14] K. A. Thompson and R. D. Ruth, Phys. Rev. D 41, 964 (1990); G. Decker and J. M. Wang, Phys. Rev. D 38, 980 (1988); D. Whittum *et al.* (to be published).

[15] D. G. Colombant, Y. Y. Lau, and D. Chernin, Part. Accel. 35, 193 (1991); Nucl. Instrum. Methods Phys. Res., Sect. A 311, 1 (1992); in *Intense Microwave and Particle Beams III*, edited by H. Brandt, SPIE Proceedings Vol. 1629 (SPIE, Bellingham, WA, 1992), p. 538.

[16] R. M. Gilgenbach, L. D. Horton, R. F. Lucey, Jr., S. Bidwell, M. Cuneo, J. Miller, and L. Smutek, in *Digest of the Fifth IEEE Pulsed Power Conference* (IEEE, New York, NY, 1985), p. 126.

[17] P. R. Menge, R. M. Gilgenbach, and R. A. Bosch, Appl. Phys. Lett. 61, 642 (1992).

[18] The epsilon factor for the TM_{110} mode is $\epsilon=0.422\times(l/L)[I(\mathrm{kA})/17]\beta/\gamma$, where l is the cavity length, L is the distance between cavity centers, I is the beam current, and β and γ are the usual relativistic velocity and mass factors. See Refs. [4] and [8] for further explanation.

[19] We should mention that these coupled-cavity effects may occur naturally in certain recirculating accelerators, as addressed in Ref. [15]. If additional loss is introduced to the main or dummy cavity, the analysis may simply be modified by assigning a lower value of Q in the operator L in Eqs. (2) and (3), and the growth rate may be assessed in a similar manner.

Microwave growth from the beam breakup instability in long-pulse electron beam experiments

P. R. Menge, R. M. Gilgenbach, and R. A. Bosch
Intense Energy Beam Interaction Laboratory, Nuclear Engineering Department, University of Michigan, Ann Arbor, Michigan 48109-2104

(Received 2 April 1992; accepted for publication 8 June 1992)

The beam breakup (BBU) instability has been investigated in high-current, long-pulse electron beams propagating through microwave cavities. Experiments are performed using a relativistic electron-beam generator with diode parameters: 0.7–0.8 MV, 1–15 kA, and 0.5–1.5 μs. The magnitude of the solenoidal magnetic field places these experiments in an intermediate regime between strong focusing and weak focusing. The electron-beam transport system consists of ten identical pillbox cavities each containing a small microwave loop antenna designed to detect the TM_{110} beam breakup mode. The TM_{110} microwave mode is primed in the first cavity by a magnetron tuned to the resonance frequency of 2.5 GHz. The BBU instability growth is measured through the amplification of the 2.5 GHz microwaves between the second and tenth cavities. Strong growth (25–38 dB) of the TM_{110} microwave signal is observed when the initial cavity is primed exactly on resonance, with a rapid decrease of the growth rate off-resonance. The magnitude of microwave growth is consistent with the predictions of BBU theory.

The beam breakup (BBU) instability is one of the most serious instabilities in high-current and long-pulse electron-beam accelerators. The BBU instability results from the coupling between the transverse motions of the electron beam and the nonaxisymmetric TM_{110} mode of the cavity structure.[1] This important instability can cause numerous effects on electron beams, such as emittance degradation, loss of current, and pulse shortening.[2,3] Recently, there has been interest in using transverse e-beam modulation to produce high-power microwaves.[4–7] While the theory of the BBU instability has been advanced considerably in recent years,[8–13] there have been few journal publications where BBU is systematically studied in experiments and compared with theories.[14]

In this letter, we study the evolution of BBU instability in a few (ten) cavity system. This problem is of interest to multicavity klystrons and magnicons,[15] and may serve as a stringent test of the continuum description of BBU in a few-cavity system. The present experimental approach utilizes a long-pulse electron beam coasting through a series of identical microwave cavities. The first cavity is primed at the TM_{110} resonance frequency by a kilowatt microwave magnetron. The parameters for these experiments place the BBU growth rate scaling close to the boundary between the weak[1] and strong focusing[9,16] regimes (defined in Ref. 3).

The electron-beam accelerator used for the experiments is the Michigan Electron Long Beam Accelerator (MELBA) with diode parameters: voltage $=-0.7$–0.8 MV, current $=1$–15 kA, and pulse length $=0.5$–5 μs, with voltage flattop provided by an Abramayan-type compensation stage over 1.5 μs.[17]

The experimental configuration is shown in Fig. 1. The electron beam is produced by a field/explosive emission button cathode. The cathode is covered with cotton velvet and is mounted on a hemispherical-end cathode stalk. The anode consists of a graphite plate located 10.8 cm from the end of the cathode. Centered in the anode is a circular aperture (2-cm diam) which extracts 40–300 A into the transport chamber. The diode chamber is immersed in a uniform solenoidal magnetic field that can be varied from 0.5–1.2 kG.

The transport chamber consists of a stainless-steel vacuum drift tube wound with solenoidal coils pulsed independently from the diode. These coils produce a quasi-dc magnetic field of up to 3.5 kG (duration $=20$ ms). Figure 1 (upper) illustrates the magnetic-field profile of the experiment. Within the drift tube are ten brass pillbox resonant cavities with a radius of 6.9 cm and a length of 2.0 cm. Inside each cavity is a small loop antenna (0.7-cm diam) oriented to be sensitive to the TM_{110} cavity mode. The average TM_{110} resonant frequency is 2.5075 ± 0.0026 GHz, and the average Q is 215 ± 45. These low-Q values were obtained by loading each cavity with a ring of microwave absorber. The cavities are separated by smaller diameter copper tubes (radius $=1.9$ cm, length $=6.5$ cm). The purpose of these tubes is to cutoff the electromagnetic propagation of the microwaves between the cavities. Thus, there is negligible cavity-to-cavity crosstalk and the system is immune to the regenerative BBU instability. The measured attenuation of the 2.5 GHz, TM_{110} microwaves is 26 dB from cavity-to-adjacent cavity.

The loop antenna in the first cavity is connected to a 1-kW level external microwave pulse generator (magnetron) to prime the cavity's TM_{110} mode. The priming microwave pulse is 3-μs long and begins before the e beam is present. In the second cavity, the e beam-induced microwave signal is received by the loop antenna and propagated out of the vacuum chamber through coaxial cable to an S-band waveguide. At the end of the waveguide, the microwave signal is attenuated and filtered for frequency information. Part of the microwave signal is diverted into a filter which passes 2.5075 ± 0.0115 GHz. The filter rejects all frequencies except that which corresponds to the TM_{110} beam breakup mode. The microwave power is measured with diode detectors. The rf in the tenth and last cavity is

 0003-6951/92/310642-03$03.00 © 1992 American Institute of Physics

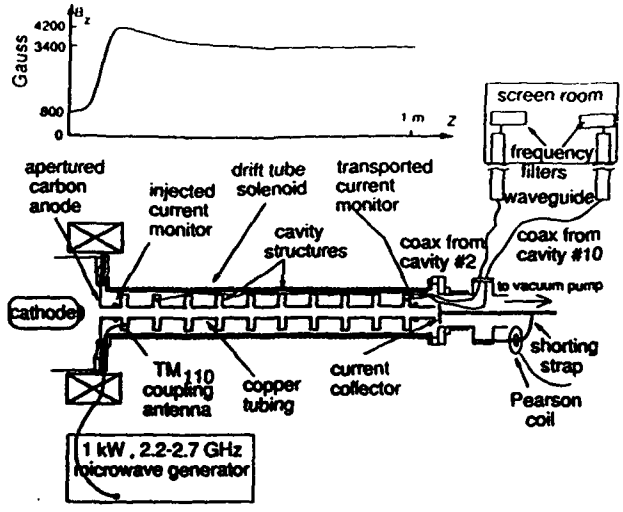

FIG. 1. Experimental configuration (lower), with typical magnetic-field profile (upper).

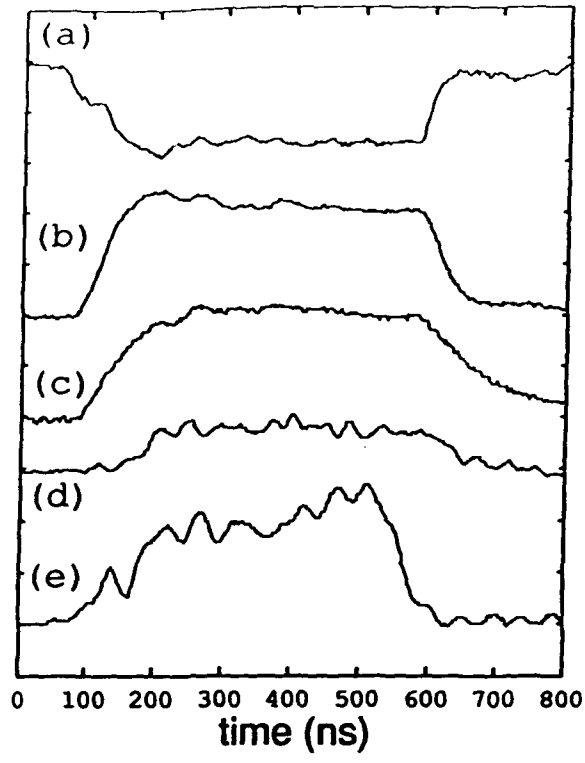

FIG. 2. Experimental data: (a) electron beam voltage (465 kV/div); (b) injected current into first cavity (92 A/div); (c) transported current leaving tenth cavity (92 A/div); (d) microwave diode detector signal in the second cavity, filtered at 2.5075±0.0115 GHz, 6-dB attenuation; (e) microwave diode detector signal in the tenth cavity filtered at 2.5075 ±0.0115 GHz, 35-dB attenuation.

measured in the same way with its own cable, waveguide, and filter. The BBU growth is determined by the decibels of growth in 2.5-GHz microwave power between the second and tenth cavities.

The beam current is measured before entering the first cavity and after exiting the last cavity using calibrated Rogowski coils. After exiting the cavity structure, the beam propagation is terminated by a copper collector plate grounded by a cable which passes through a Pearson current transformer.

Figure 2 depicts typical experimental data. The uppermost trace (a) is the MELBA diode voltage in which the flattop occurs at 750 kV and lasts for 600 ns. The second signal (b) is the current entering the first cavity with a peak which corresponds to 200 A. Signal (c) is the current exiting the tenth cavity, and the peak corresponds to 190 A. The fourth signal (d) is the microwave power signal in the second cavity after being filtered at 2.5 GHz; the signal has been attenuated by 6 dB. The lowermost signal (e) is the microwave power in the tenth cavity after being filtered at 2.5 GHz; this signal has been attenuated by 35 dB. Allowing for the difference in signal amplitudes and detector sensitivities, the growth of the 2.5-GHz microwaves is measured to be about 36 or 4.5 dB per cavity. These data were taken at a solenoidal magnetic field of 3.4 kG.

The theoretical magnitude of beam breakup instability growth can be obtained by calculating the imaginary wavenumber in the BBU dispersion relation. If the continuum theory[3,18] is used the appropriate dispersion relation is

$$(\Omega^2-\omega_c\Omega+\Gamma)(\Omega^2+\omega_c\Omega+\Gamma)=0, \tag{1}$$

where, $\Omega=\omega-vk$

$$\Gamma=\frac{2\omega_0^4\epsilon}{-\omega^2+\omega_0^2+i\omega\omega_0/Q},$$

ω_c is the relativistic betatron frequency, ω is the frequency of the beam breakup wave, v is the velocity of the electron beam, k is the wavenumber, ω_0 is the angular frequency of the TM_{110} mode, Q is the quality factor of the cavity, and ϵ is the dimensionless coupling factor.[19] Using the data from Fig. 2, the calculated BBU growth is 34 dB.

If the betatron wavelength or the BBU e-folding length does not greatly exceed the spacing of the accelerator cavities, then the transverse impulsive forces from the cavities can no longer be treated as a continuous force per unit length. If this condition exists, then a continuum model may be inappropriate, and a model treating the cavities as discrete entities would be more applicable. This is the case here, for the betatron wavelength of the MELBA beam at 3.4 kG is 7.8 cm, and the cavity spacing is 8.5 cm. Thus, a more accurate dispersion relation is[20]

$$k(\omega)=\frac{\omega}{v}\pm\frac{\omega_c}{2v}-\frac{1}{L}\arccos\left(\cos\frac{L\omega_c}{2v}+\frac{\Gamma L}{\omega_c v}\sin\frac{L\omega_c}{2v}\right), \tag{2}$$

where L is the distance between adjacent cavity centers. Using the data from Fig. 2, the calculated growth rate is 35 dB for the discrete-cavity asssumption.

Figure 3 shows the 2.5-GHz microwave signal growth plotted for various values of I/B (I/B is the ratio of transported current to the magnetic field). The theoretical BBU growth rate is approximately linearly proportional to I/B. The solid circles are experimental data which were obtained by varying the magnetic field. The open circles are the discrete-cavity [Eq. (2)] theoretical growth points as calculated from the parameters of the corresponding ex-

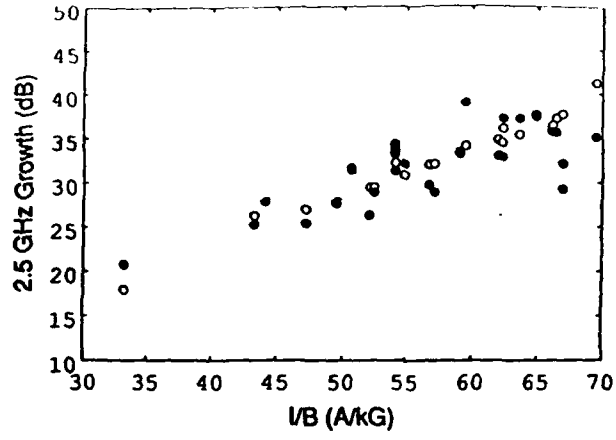

FIG. 3. Microwave growth (2.5 GHz) dependence on the current to magnetic-field ratio, I/B. The filled circles are experimental data and the open circles are theoretical predictions calculated by the discrete-cavity theory [Eq. (2)] from the corresponding experimental points with the same I/B.

perimental points. The values of ϵ for the plotted points range from 5.6×10^{-5} to 5.2×10^{-4}. The agreement between theory and experiment is excellent at low currents. The larger difference between theory and experiment at higher currents could be due to e-beam-induced detuning of the cavity resonance from its cold-test value.[14]

Figure 4 shows the effect of priming the first cavity at frequencies other than its exact TM_{110} mode resonant frequency. The plotted points are experimental data taken at the same magnetic field (3.4 kG) and nearly the same e-beam current (190–215 A). The solid curve is the BBU growth as predicted by the discrete-cavity equation (2) using $I=210$ A and letting ω vary as the priming angular frequency. The dashed curve is the continuum BBU growth equation (1) for the same parameters. This experimental data is strongly peaked near the central TM_{110} resonant frequency of 2.5075 GHz, showing that this

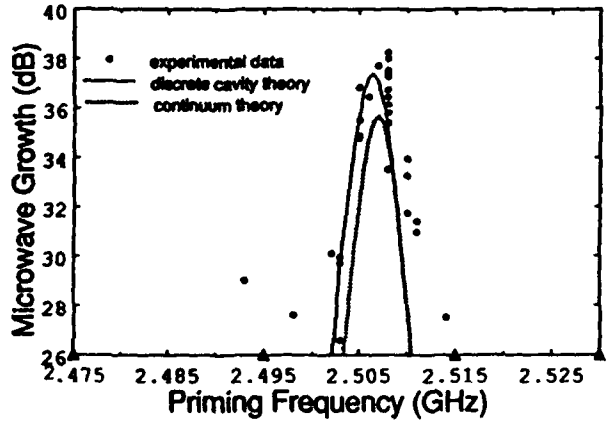

FIG. 4. Microwave growth dependence on the frequency of microwaves injected into the first cavity. The filled circles are experimental data. The solid curve is the theoretical growth predicted by the discrete-cavity mode coupled theory, Eq. (2) (see Ref. 20). The dashed curve is the theoretical growth predicted by the continuum cavity mode coupled theory, Eq. (1) (see Refs. 3 and 18). The triangles along the abscissa indicate experimental growth below the level of detectability (i.e., below 26 dB).

mode, and thus, the beam breakup instability, is responsible for the observed microwave growth. It should be noted that the experimental beam breakup instability growth more closely follows the discrete-cavity theory than the continuum theory. This is expected because the continuum theory assumes that the distance between cavities is negligible compared to the betatron wavelength and the BBU e-folding length. For this experiment, both the betatron wavelength and the e-folding length are comparable to the distance between cavity centers.

In conclusion, the beam breakup instability has been experimentally studied for the difficult regime of intermediate focal strength. The adequacy of the continuum BBU description for few-cavity systems is tested, even under conditions where the betatron wavelength is comparable to the cavity spacing. Strong instability growth is only found by microwave priming at the resonance frequency of the TM_{110} microwave mode, a characteristic of the beam breakup instability.

We appreciate valuable discussions with Y. Y. Lau. We acknowledge the experimental assistance of P. L. G. Ventzek, C. H. Ching, M. Walter, J. Foster, and T. Spencer. This research was supported by SDIO-IST through an ONR contract.

[1] W. K. H. Panofsky and M. Bander, Rev. Sci. Instrum. 39, 206 (1968).
[2] R. Helm and G. Loew, *Linear Accelerators*, edited by P. M. Lapostelle and A. L. Septier (North Holland, Amsterdam, 1970), Chap. B.1. 4, p. 173.
[3] Y. Y. Lau, Phys. Rev. Lett. 63, 1141 (1989).
[4] B. B. Godfrey, D. J. Sullivan, M. J. Arman, T. C. Genoni, and J. E. Walsh, Proc. SPIE Int. Soc. Opt. Eng. 1061, 84 (1989).
[5] T. J. T. Kwan, M. A. Mostrom, and B. B. Godfrey, Phys. Rev. Lett. 66, 3221 (1991).
[6] P. J. Tallerico, IEEE Electron Devices ED-26, 1559 (1979).
[7] R. J. Adler, J. R. Bayless, S. Humphries, Jr., and George A. Proulx, Pulse Sciences, Inc., San Leandro, CA, Report PSI-FR-2293-1 (1988).
[8] V. K. Neil and R. K. Cooper, Part. Accel. 1, 111 (1970).
[9] V. K. Neil, L. S. Hall, and R. K. Cooper, Part. Accel. 9, 213 (1979).
[10] A. W. Chao, B. Richter, and C. Y. Yao, Nucl. Instrum. Methods 178, 1 (1980).
[11] R. L. Gluckstern, R. K. Cooper, and P. J. Channell, Part. Accel. 16, 125 (1985).
[12] D. G. Colombant and Y. Y. Lau, Appl. Phys. Lett. 55, 27 (1989).
[13] C. L. Bohn and J. R. Delayen, in Conference Record of *1991 IEEE Particle Accelerator Conference*, IEEE Catalogue No. 91 CH3038-7, 3, 1809 (1991).
[14] P. R. Menge, R. M. Gilgenbach, R. A. Bosch, H. Ching, T. A. Spencer, and M. Walter, Proc. SPIE 1629, 529 (1992).
[15] S. Gold (private communication).
[16] G. J. Caporaso, F. Rainer, W. E. Martin, D. S. Prono, and A. G. Cole, Phys. Rev. Lett. 57, 1591 (1986).
[17] R. M. Gilgenbach, L. D. Horton, R. F. Lucey, Jr., S. Bidwell, M. Cuneo, J. Miller, and L. Smutek, in *Digest of the 5th IEEE Pulsed Power Conference* (IEEE, New York, NY, 1985), p. 126.
[18] R. A. Bosch and R. M. Gilgenbach, Appl. Phys. Lett. 58, 699 (1991).
[19] The epsilon factor for the TM_{110} mode is $\epsilon=0.422(l/L)[I(kA)/17](\beta/\gamma)$, where l is the cavity length, L is the cavity spacing, I is the beam current, and β and γ are the usual relativistic velocity and mass factors. See Refs. 3 and 12 for further explanation.
[20] R. A. Bosch, P. R. Menge, and R. M. Gilgenbach, J. Appl. Phys. 71, 3091 (1992).

Beam Breakup Instability in an Annular Electron Beam

Y. Y. Lau and John W. Luginsland
Intense Energy Beam Interaction Laboratory
and
Department of Nuclear Engineering
University of Michigan
Ann Arbor, MI 48109-2104

Abstract

It is shown that an annular electron beam may carry six times as much current as a pencil beam for the same beam breakup (BBU) growth. This finding suggests that the rf magnetic field of the breakup mode is far more important than the rf electric field in the excitation of BBU. A proof-of-principle experiment is suggested, and the implications explored.

Annular electron beams have the capability of carrying a much higher current than a pencil beam. Besides the obvious fact that annular beams have a larger cross-sectional area, their limiting currents are significantly higher than those of a pencil beam when placed in a metallic drift tube. For this and other reasons, annular beams have recently been chosen as the preferred geometry to generate coherent, ultra-high power microwaves.[1,2] They have also been used as the primary beam in several "two-beam accelerator" configurations.[3,4] These annular beams either encounter a sequence of modulating gaps, or simply glaze by a slow wave structure to generate a wake field in the case of two-beam accelerators.[3] Their high current may then lead to the beam breakup instability (BBU)[5-9] and this concern motivates the present study.

BBU is usually analyzed for a pencil beam propagating along the center axis of a sequence of accelerating cavities. Many BBU calculations of practical interest assume that the accelerating unit is the familiar cylindrical pillbox cavity and that the dominant deflecting mode is the TM_{110} mode.[5,6,9] Extension to an annular beam is straightforward. Nevertheless, this calculation leads to several unexpected results and provides some new insights into BBU, to be reported in this paper.

It is well known that BBU is excited by the combined action of the rf magnetic field (B_1) and the rf electric field (E_1) of the deflecting mode[5]: B_1 causes beam deflection through the Lorentz

force and E_1 causes mode amplification through the work done on the mode by the beam current J. Our calculation strongly suggests that B_1 is much more critical than E_1 in contributing to BBU growth. Thus, an annular beam strategically placed near the minimum of the rf magnetic field would suffer far less beam breakup growth than a pencil beam that is centered on the cavity axis, where the magnetic field is large and the axial electric field is small. By the same argument, placing the annular beam very close to the wall of a metallic drift tube, at which the axial electric field is vanishingly small, cannot eliminate BBU growth because of the substantial deflecting magnetic field generated by the wall current. Toward the end of this paper, we propose an experiment which would unambiguously test the relative importance between the rf magnetic field and the rf axial electric field, as discussed here.

Consider an infinitesimally thin annular beam of radius r_o inside a cylindrical drift tube of radius b. The beam carries a total current I and coasts at velocity v_o with the corresponding relativistic factors γ and β. The drift tube is loaded with a slow wave structure, modeled by a series of cylindrical pillbox cavities, each of which supports the nonaxisymmetric TM_{110} mode.[3,5,6,9] The interaction between this mode and the beam causes BBU to be excited. In the limit $r_o \to 0$, this is the basic model of BBU for a pencil beam. Since we are comparing the strength of BBU interaction for different values of r_o, we pretend that magnetic focusing is absent and that the quality factor Q of the deflecting mode is infinite.

Let $A_1 = \hat{z}\, q(t)\, (\cos\theta)\, E(r)$ be the vector potential of the deflecting dipole mode in a cavity. For the fundamental TM_{110} mode, $E(r) = J_1(pr)$ represents the radial dependence of the axial electric field with J_1 being the Bessel function of order one and $p = 3.832/b$. The corresponding magnetic field is $B_1 = \nabla \times A_1$. The action of this mode on the beam is calculated as follows.

We divide the annular beam into N azimuthal segments (N large). The i-th segment is located at $r=r_o$, $\theta = \theta_i = 2\pi\, i/N$, in the unperturbed state but is displaced radially by ξ_i and azimuthally by η_i when the deflecting mode is present. The linearized force law yields

$$-\gamma(\omega - kv_o)^2 \xi_i = (e/m_o)(v_o/c) q E'(r_o) \cos\theta_i \qquad (1)$$

$$-\gamma(\omega - kv_o)^2 \eta_i = -(e/m_o)(v_o/c) q [E(r_o)/r_o] \sin\theta_i \qquad (2)$$

where the right hand sides represent the components of the Lorentz force that causes beam deflection. In writing Eqs. (1) and (2), we have assumed a wave-like solution $\exp[j(\omega t - kz)]$ for the disturbances, with $j^2 = -1$, and we have used a prime to denote derivative with respect to the argument.

The instantaneous current J on the i-th current filament is

$$\vec{J}_i(r,t) = \hat{z}\, \frac{I}{N} \frac{1}{r} \delta(r - r_o - \xi_i)\, \delta\left(\theta - \theta_i - \frac{\eta_i}{r_o}\right) \qquad (3)$$

where δ is the Dirac delta function. The work done by this current filament on the deflecting mode is proportional to

$$W_i = \int dV \quad \vec{A_1} \bullet \vec{J_i} \tag{4}$$

where the volume integral is performed over the cavity. In evaluating W_i , we should retain only the rf component of J_i in Eq. (3), since only the rf current performs work on the breakup mode. Upon substituting Eqs.(1)-(3) into Eq.(4), and summing over all i, we find the total work done

$$W = \sum_{i=1}^{N} W_i = \frac{LIe}{m_o} \frac{v_o}{c} q \frac{\left[E'(r_o) \right]^2 + \left[E(r_o)/r_o \right]^2}{\gamma(\omega - kv_o)^2} \tag{5}$$

apart from a multiplicative constant that is independent of the beam's equilibrium position r_o . This energy transfer leads to growth of the BBU mode, which is described by the BBU dispersion relation:[8]

$$\left(\omega^2 - \omega_o^2\right)\left(\omega - kv_o\right)^2 = -2\omega_o^4\varepsilon = -2\omega_o^2\varepsilon_o\left(\frac{\varepsilon}{\varepsilon_o}\right) \tag{6}$$

where ε is the coupling constant and ω_o is the breakup mode frequency. In writing the last form of Eq. (6), we normalize ε in terms of ε_o , the coupling constant for an on-axis, pencil beam

($r_o \to 0$). For the TM_{110} mode, $E = J_1(pr)$ and $\varepsilon_o = 0.422(\beta/\gamma)(I/1kA)$. It is clear from Eq. (5) that

$$\frac{\varepsilon}{\varepsilon_o} = 2\left\{\left[J_1'(pr_o)\right]^2 + \left[\frac{J_1(pr_o)}{pr_o}\right]^2\right\} \qquad (7)$$

which compares the BBU strength between an annular beam and a pencil beam of the same current. Note that this ratio reduces to unity in the limit $r_o \to 0$.

Equation (7) is plotted in Fig. (1) as a function of r_o/b. It is seen from this figure that $\varepsilon/\varepsilon_o$ may be as small as 0.17 when the annular beam is located at $r_o \approx 0.56b$. Note also that this location coincides with the minimum of the rf magnetic field of the deflecting mode. What this means is that an annular beam placed at this location can carry as much as $1/0.17 = 6$ times the current as an on-axis pencil beam, and suffer the same BBU growth. Another point worth noting is that BBU growth retains significant strength even if the annular beam is very close to the wall of the drift tube [cf. $r_o \to b$ in Fig. (1)]. This result is unexpected since $E_1 \to 0$ near a metallic wall. As a result, $J_1 \bullet E_1 = 0$ and there would be little transfer of power from the beam to drive the breakup mode. The finite BBU strength as $r_o \to b$ is another strong indication that the deflecting magnetic field is far more important than the axial rf electric field in driving BBU.

The importance of the rf magnetic field can be tested in an experiment in which a pencil beam is focused by a solenoidal magnetic field and is made to pass through a sequence of pillbox cavities, in which the first cavity is primed with microwaves at the TM_{110} mode.[9] BBU growth is monitored at the last cavity, before the beam exit. The above theory then predicts the unusual feature that BBU growth should be much less if the pencil beam is placed off-axis, than if the pencil beam were on-axis.[10] The BBU growth should be minimum if this pencil beam is placed at a distance of about 0.56 of the pillbox radius, where the rf magnetic field is minimum.

We also repeated the calculations for the higher order radial modes: TM_{120}, TM_{130}, TM_{140}, and TM_{150}. Fixing $r_o/b \approx 0.56$, the ratio $\varepsilon/\varepsilon_o$ equals 0.16, 0.012, 0.037, and 0.013 for these four higher order modes, respectively. Thus, the annular beam still suffers substantially lower BBU growth, in the higher order deflecting modes, than an on-axis pencil beam of the same current.

In conclusion, the rf magnetic field is found to be much more important than the rf electric field in contributing to BBU growth. A simple proof-of-principle experiment is proposed to test this new finding. Annular beams are far more stable than an on-axis pencil beam, as a result.

We thank Professor Ronald Gilgenbach for his support and for many useful discussions. This work was supported in part by an SDIO/IST contract managed by ONR.

References

1. V. Serlin and M. Friedman, Appl. Phys. Lett., to be published; Y.Y. Lau, M. Friedman, J. Krall, and V. Serlin, IEEE Trans. PS-18, 553 (1990) and references therein; M. Friedman, Y.Y. Lau, J. Krall, and V. Serlin, U.S. Patent 5,132,638 (issued July 21, 1992); J. Krall, M. Friedman, Y.Y. Lau, and V. Serlin, IEEE Trans. EMC-34, p.22 (1992).

2. C. Chen, P. Catraras, and G. Bekefi, Appl. Phys. Lett., (1993); See also, "Intense Microwave and Particle Beams III," Proc. SPIE 1629, Ed. H. Brandt (1992).

3. G. Voss and T. Weiland, DESY Reports M82-10 (1982); M82-079 (1982).

4. M. Friedman, J. Krall, Y.Y. Lau, and V. Serlin, Phys. Rev. Lett. 63, 2468 (1989).

5. W.K.H. Panofsky and M. Bander, Rev. Sci. Instrum. 39, 206 (1968); R.H. Helm, and G.A. Loew, in Linear Accelerators, eds. R.P. Lapostolle, and A.L. Septier. (North-Holland, Amsterdam, 1970), p.173.

6. V.K. Neil, L.S. Hall, and R.K. Cooper, Part. Accel. 1, 111 (1970); 9, 213 (1979).

7. A.W. Chao, B. Richter, and C.Y. Yao, Nucl. Instrum. Methods. 178, 1 (1980); K.A. Thompson and R.D. Ruth, Phys. Rev. D41, 964 (1990); R.L. Gluckstern et. al., Part. Accel. 23, 37 (1988); C.L. Bohn, and J.R. Delayen, Phys. Rev. A45, 5964 (1992); D. Chernin, and A. Mondeli, Part. Accel. 24, 685 (1985); G. Decker, and J.M. Wang, Phys. Rev. D38, 980 (1988); G. Caporaso et. al., Phys. Rev. Lett. 54, 685 (1985); D. Colombant, Y.Y. Lau, and D. Chernin, Part. Accel. 35, 193 (1991).

8. Y.Y. Lau, Phys. Rev. Lett. 63, 1141 (1989).

9. P.R. Menge, R.M. Gilgenbach, and Y.Y. Lau, Phys. Rev. Lett. 69, 2372 (1992); P.R. Menge et al., Appl. Phys. Lett. 61, 642 (1992).

10. BBU growth on a pencil beam that is placed off-center can be easily calculated by using Eq. (4) instead of Eq. (5). We pretend that the total beam current is carried by the i-th filament that enters Eq. (4). Although the BBU growth of such an off-center beam depends on θ_i, its coupling constant ε is still much less than ε_o, the value for an on-axis beam.

Figure Caption

Fig. 1. Comparison of the BBU coupling constant ε between an annular beam of radius r_o and an on-axis pencil beam ($r_o \rightarrow 0$) with the same total current.

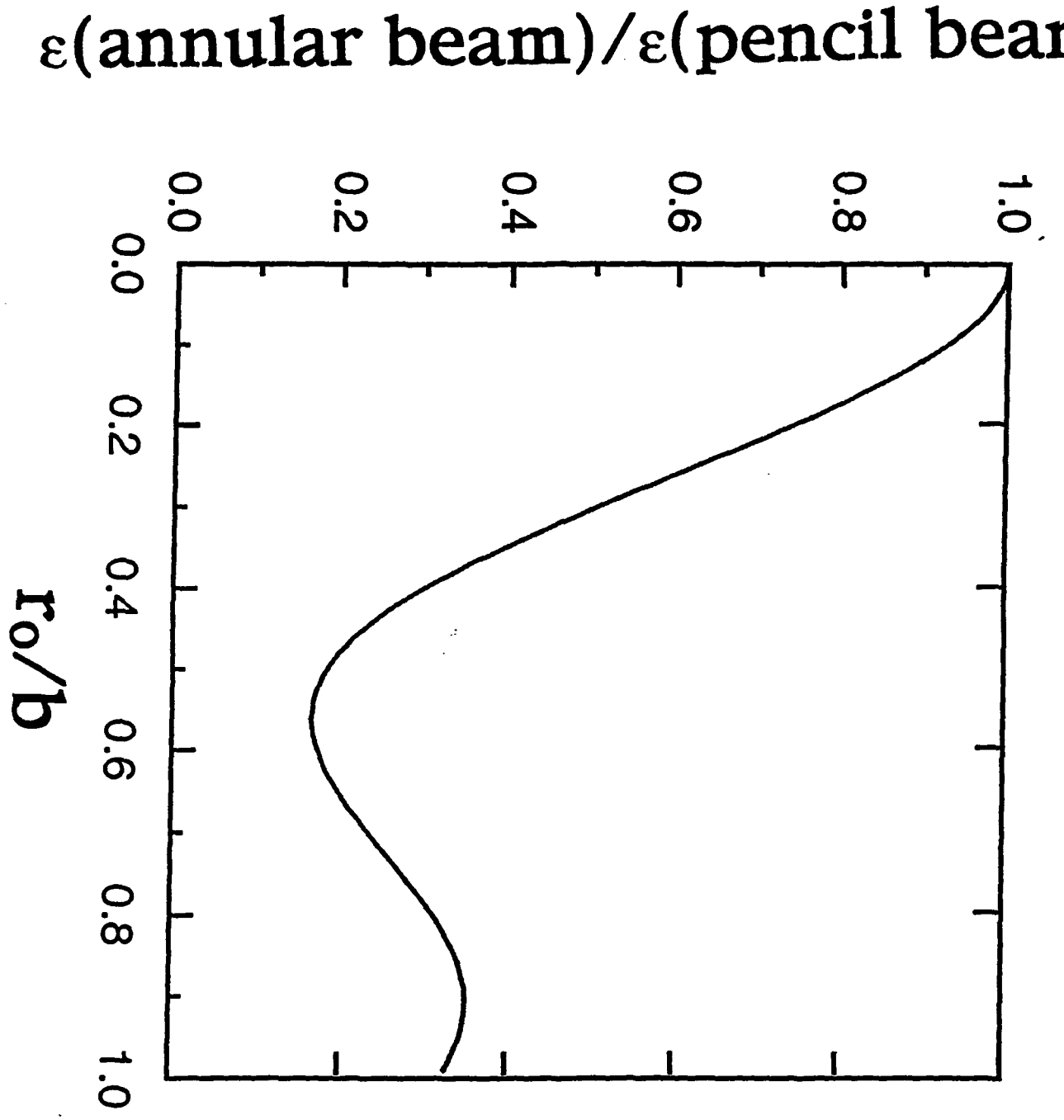
ε(annular beam)/ε(pencil beam)
0.0
0.2
0.4
0.6
0.8
1.0
ro/b
0.0
0.2
0.4
0.6
0.8
1.0

Fig. 1

Beam breakup growth and reduction experiments in long-pulse electron beam transport

P.R. Menge†, R.M. Gilgenbach, Y.Y. Lau, and R.A. Bosch*
Intense Energy Beam Interaction Laboratory, Nuclear Engineering Department, University of Michigan, Ann Arbor, Michigan 48109-2104

The results of an experimental program whose sole objective is to investigate the cumulative beam breakup instability (BBU) in electron beam accelerators is presented. The BBU growth rate scalings are examined with regard to beam current, focusing field, cavity Q, and propagation distance. A microwave cavity array was designed and fabricated to excite and measure the cumulative BBU resulting from beam interactions with the deflecting TM_{110} cavity mode. One phase of this experiment used high Q ($\approx$ 1000) cavities with relatively large frequency spread ($\frac{\Delta f}{f_o} \approx 0.1$ %). The observed TM_{110} mode microwave growth between an upstream (2^{nd}) and a downstream (10^{th}) cavity indicated BBU growth of 26 dB for an electron beam of kinetic energy of 750 keV, 45 A, and focused by a 1.1 kG solenoidal field. At beam currents of less than 100 A the experiments agreed well with a two-dimensional continuum theory; the agreement was worse at higher beam currents (>100A) due to beam loading. The second phase experiments used lower Q ($\approx$ 200) cavities with relatively low frequency spread ($\frac{\Delta f}{f_o} \approx 0.03$ %). Theory and experiment agreed well for beam currents of up to 220 A.

Instability growth reduction experiments using the technique of external cavity coupling resulted in a factor of four decrease in energy in BBU growth when seven internal beam cavities were coupled by microwave cable to seven identical external dummy cavities. A theory invoking power sharing between

---

† Present address: Sandia National Laboratories, Dept. 1231, Albuquerque, NM 87185
* Present address: Synchrotron Radiation Center, University of Wisconsin-Madison, Stoughton, WI 43589-3097

the internal beam cavities and the external dummy cavities was used to explain the experimental reduction with excellent agreement using an equivalent circuit model.

PACS numbers: 41.80.Ee, 41.70.+t, 52.70.Gw

I. INTRODUCTION

The beam breakup instability (BBU) is one of the most serious of the electron beam instabilities that arise in linear accelerators[1]. This instability results from the coupling of transverse beam oscillations and nonaxially symmetric electromagnetic modes of the accelerating structure. The beam breakup instability can be classified into two major categories, regenerative and cumulative. In the regenerative BBU, upstream (backward) propagation of the nonaxially symmetric mode provides feedback for amplification within a single accelerator section [2]. In the cumulative (also called multisection) BBU instability, the nonaxially symmetric modes of different accelerator sections are coupled only by the passage of the electron beam. The study presented in this paper will deal exclusively with the cumulative BBU. The BBU is capable of growing over time in one cavity as the trailing portions of the beam become more severely deflected than the proceeding portions. This instability can also grow over distance as the amplifying disturbances are carried along the beam, resulting in a range of macroscopic effects, from simple degradation of beam quality (emittance growth) to total loss of beam current if the beam strikes the cavity walls. BBU therefore places a limit on the beam's pulselength, propagation distance, and the beam current.

Despite the serious limitations imposed on accelerators by the BBU, there have been few publications where BBU is systematically studied in experiments and compared with the theories. The goal of the experiments presented in this paper is to systematically study the experimental scaling laws and growth rates for the beam breakup instability. This work is the first experiment designed whose sole objective is to investigate the behavior of the BBU. With this goal in mind, the experimenter is free to investigate parameters that have limited variability in large scale accelerator programs. These parameters include beam current, focusing magnetic field, pulselengths, cavity Q, and BBU frequency. A summary of some of these University of Michigan experiments can be found in Ref. 3. A second objective is to develop novel techniques to reduce

the growth of the BBU. One such technique performed during the course of this research is the demonstrated use of "external cavity coupling" [4].

The experimental approach proceeded in three phases. The first experiments examined the growth of the BBU using an approximately 1 meter long array of RF resonant pillbox cavities characterized by relatively high Q (≈ 1000) and moderately large frequency spread ($\Delta f/f \approx 0.1$ %) among the cavities. These high Q experiments demonstrate the importance of beam loading. To reduce the effects of beam loading, in the next phase, we employed a cavity array with a lower Q (≈ 200), but the frequency spread was much smaller ($\Delta f/f \approx 0.03$ %). Two subsets of these latter experiments were performed investigating BBU behavior over beam propagation distances of 1 m and 2 m. The parameters for these experiments place the BBU growth rate scaling close to the boundary between the weak [1] and strong focusing [5,6] regimes (defined in Ref. 7). The third phase consisted of experiments designed to reduce the BBU growth rate using the aforementioned external cavity coupling.

A useful comparison of MELBA growth rate scalings to those of other well-known accelerators is shown in Figure 1. As explained in Ref. 7, the parameter S1 is proportional to beam current, and inversely proportional to the square of the applied focusing field, and S3 is the ratio of accelerator length normalized by the betatron wavelength to the pulselength normalized by the period of the deflecting mode. Each region on the graph represents a unique BBU growth rate scaling defined in Ref. 7.

II. HIGH Q, LARGE FREQUENCY SPREAD EXPERIMENTS.

The electron beam accelerator used in this research is the Michigan Electron Long Beam Accelerator (MELBA). The MELBA diode operates with the following parameters: voltage = -0.7 to -0.8 MV, diode current = 1 - 10 kA, and pulselength = 0.3 - 5 μs, with flattop voltage provided by an Abramyan type compensation stage over 1 μs.

The experimental configuration is shown in Figure 2. The electron beam is generated from an explosive emission velvet cathode. This cathode consists of a glyptal coated hemispherical-end cathode stalk with a velvet emitting button attached to the end of the cathode stalk. This cathode is advantageous for its slow diode closure, limited edge emission, and relatively long glyptal life. The anode is a graphite plate (1/8 " thick) located 10.8 cm from the end of the cathode. A circular aperture with a diameter of 2 cm is centered on the anode plate to extract 40-300 A into the transport chamber.

The diode chamber is immersed in a solenoidal magnetic field that can be varied from 0.5 - 1.2 kG. The transport chamber is composed of a 1 m long drift tube surrounded by solenoid coils pulsed independently from the diode. The current to the solenoid is provided by a 2-stage, double-polarity, electrolytic capacitor bank that produces a magnetic field up to 3.5 kG. Since the diode coils and the drift tube solenoid overlap, the superposition of the solenoidal fields causes a total B-field profile that is not quite uniform in the experimental chamber. The profile is higher on the upstream end before tapering to a flattop about halfway down the drift tube.

Within the drift tube are ten brass pillbox resonant cavities separated by smaller diameter copper tubes. Each cavity has a radius of 6.9 cm and a length of 2.0 cm. Within each cavity is a small loop antenna oriented to be sensitive to the TM_{110} cavity mode. With cylindrical pillbox cavities, the TM_{110} mode is the most significant beam breakup mode, because it is the fundamental, nonaxially symmetric mode, and it produces the maximum instability growth. The length of the separation tubes is 6.5 cm, giving an intercavity distance of 8.5 cm. The diameter of the tubes is 3.8 cm, which is below the TM_{010} cutoff diameter, and thus serves to isolate each cavity from RF crosstalk. The measured attenuation of the ≈ 2.5 GHz, TM_{110} mode microwaves is 26 dB from cavity to adjacent cavity. This ensures that the BBU under study is the cumulative type (i.e. non-regenerative type).

The first cavity (closest to the anode) has its TM_{110} mode primed externally by an Epsco (model PG5KB) microwave pulse generator. The priming microwave pulse is generally 3 μs long

and begins before the e-beam is present. The power of the injected microwaves is generally 1 kW. The purpose of this procedure is to provide some initial transverse modulation to the beam.

The general technique used in these experiments is to investigate the beam-breakup instability by taking measurements on the characteristic microwaves produced by the instability. In particular the magnitude of BBU growth is determined through the growth of the TM_{110} microwaves between the second and tenth cavities.

In the second cavity the e-beam-induced RF is measured via the loop anter The microwaves are propagated out of the experimental chamber through RG/.405 U semi-rigid transmission cable to a vacuum feedthrough, to RG/8 cable, to an S-band waveguide. The waveguide runs to a Faraday cage where the signal is attenuated and filtered for frequency information. Part of the microwave signal is diverted into a filter that passes 2.5 GHz ± 11 MHz. This frequency, as noted above, corresponds to the TM_{110} beam breakup frequency.

The RF power in the tenth (last) cavity is measured in the same way with its own set of cables and waveguide. The growth of the BBU instability is determined by the decibels of growth in 2.5 GHz microwave power between the second and tenth cavities.

Electron beam current is measured at several points in the transport experiment. Cathode stalk current in the diode is measured by a B-dot loop in the MELBA oil tank, behind the insulators. Extracted current is monitored by a Rogowski coil in the flange after the anode. Injected current is measured by a Rogowski coil before the first cavity and exit current is detected by a Rogowski coil after the last cavity. Exiting current is also measured by a carbon plate/current collector which is grounded by a strap which passes through a Pearson current transformer.

The exact TM_{110} resonant characteristics of the ten cavities in the transport array are listed in Table 1. The cavities are numbered in order of beam encounter. As indicated, the average resonant frequency is 2.523 GHz ± 0.1 %, and the average Q is 1000 ± 310. Comparison of the frequency spread ($\Delta f/f = 0.1$ %) and average resonant linewidth ($1/Q = 0.1$ %) reveals that they are approximately equal, and thus the frequency spread among the cavities can be referred to as large.

Figure 3 shows a typical data set of electron beam and RF signals from a high Q, large-frequency-spread BBU transport experiment. The uppermost signal trace (a) is the voltage applied to the diode by the MELBA Marx generator. The voltage has a total length of about 700 ns and the duration of the flattop is about 400 ns. The voltage magnitude at the flattop is -750 kV. The second trace (b) is the signal from the Rogowski coil that encircles the entrance to the first cavity. This signal has a flattop amplitude corresponding to approximately 220 A. The center trace (c) represents the transported current. This trace is the signal from the Pearson coil that surrounds the cable which connects the collector plate to ground. The magnitude of beam current on the flattop for this signal is 46 A. The drift tube solenoid produced a magnetic field of 1100 G for this particular shot. The fourth trace (d) is the diode crystal detector signal of the microwaves picked up by the loop antenna in the second cavity. This signal has passed through the frequency filter which passes frequencies at 2.523 ± 11 GHz. The external attenuation added to the second cavity microwaves is 12 dB. The lowermost trace (e) is the microwave crystal detector signal as received by the loop antenna in the tenth (last) cavity; this signal has passed through a frequency filter similar to that used for the second cavity diagnostics. The external attenuation added for this signal is 32 dB. The external microwave priming source was tuned to the exact resonance of the first cavity (see Table 1), 2.519 GHz, and the power of the priming pulse was approximately 1 kW.

The experimental spatial growth rate for the beam breakup instability can be determined from the data presented in Fig. 3. The coefficients to insert into the theoretical equations predicting the BBU growth rate can also be determined from the data. The experimental growth rate is ascertained through examination of the RF signals (traces (d) and (e) from Fig. 3). These traces are diode crystal detector signals which give measurements of microwave power injected into the detectors. Scrutiny of the microwaves from the second cavity (signal (d) of Fig. 3) shows a detector signal of about 80 mV along the flattop of the MELBA voltage pulse. A signal magnitude of 80 mV corresponds to a power of 9 mW for this particular detector. Before entering the detector, the signal was purposely reduced by 12 dB in external attenuation and also by another 2.7 dB from resistive and insertion losses in the cable, waveguide, and frequency filter. Thus, the

total power of the TM_{110} microwaves on the flattop picked up by the loop antenna in the 2nd cavity is 270 mW.

The TM_{110} microwave signal in the tenth cavity has a magnitude of about 160 mV on the flattop. Note that the overall shape of the tenth cavity microwave power is similar to that of the second cavity. There is about 40 ns of delay between the tenth and second cavity signals due to a longer waveguide used to transport the microwaves from the tenth cavity. This suggests that the magnitude of the microwaves in the tenth cavity is a direct result of growth from the second cavity microwaves. This detector's calibration at 160 mV gives a detector power of 35 mW. The added attenuation in this signal is 32 dB with an additional reduction of 2.9 dB from resistive and insertion losses. Thus, the total power received by the antenna in the tenth cavity is 99 W. Therefore, the growth in TM_{110} microwave power between the second and tenth cavities as sampled by the loop antennas is: $\frac{99\ W}{0.27\ W} \approx 370$, which is equivalent to 26 dB. The distance between the antennas is 68 cm, giving a spatial microwave growth rate of 38 dB/m.

A theoretical prediction for the amount of BBU growth can be found using the continuum dispersion relation [7-9] for solenoidal focusing [10]:

$$(\Omega^2 - \omega_c\Omega + \Gamma)\,(\Omega^2 + \omega_c\Omega + \Gamma) = 0\ , \qquad (1)$$

where $\Omega = \omega - k\,v$ and $\Gamma = \frac{2\omega_o{}^4\varepsilon}{-\omega^2 + \omega_o{}^2 + i\omega\,\omega_o/Q}$. The variable k is the wavenumber of the instability, ω is the frequency which undergoes BBU growth, ω_o is the TM_{110} angular resonant frequency, v is the electron beam velocity, Q is the cavity quality factor, ω_c is the relativistic angular betatron frequency, and ε is the dimensionless coupling constant [7], where $\varepsilon = 0.422\,\frac{\ell}{L}\,\frac{I}{17kA}\,\frac{\beta}{\gamma}$. Here, ℓ is the cavity length, L is the spacing of cavity centers, I is the e-beam current, and β and γ have their usual meanings. Using the experimental parameters of ℓ = 2 cm, L= 8.5 cm, transported current = 46 A., and kinetic energy = 750 keV finds $\varepsilon = 1.0 \times 10^{-4}$. A solenoidal field of 1.1 kG yields ω_c = 7.85 gigaradian/s, the BBU frequency is the priming frequency, $\omega = 2\pi \times 2.519$ GHz, and the average TM_{110} frequency is $\omega_o = 2\pi \times 2.523$ GHz. Insertion of these values into Eq. (1) produces a theoretical spatial growth rate in the continuum model of

$$\mathrm{Im}(k) = 4.90\ m^{-1}$$

Thus, the e-folding length for the instability is 20.4 cm. This implies an RF amplitude growth over the 68 cm between the second and the tenth cavities of $\exp\left\{\frac{68.0}{20.4}\right\} = 28.0$. An amplitude growth of 28 calculates to be 29 dB. Thus, the two-dimensional continuum theory predicts 29 dB of BBU growth for a 750 keV electron beam with current = 46 A, and a solenoidal focusing field of 1.1 kG. This is in reasonably good agreement with the experimental growth of 26 dB, considering the use of a continuous model for the few cavity system and the neglect of beam loading and frequency detune among the cavities.

The preceding continuum model treats the transverse impulsive forces from the accelerating cavities as a continuous force per unit length. This approximation limits the dispersion relations to the cases where instability scale lengths (i.e. *e* folding length, and wavelength of the BBU disturbance) are long compared to the cavity spacing. Modeling the transverse force on the beam resulting from pillbox cavities placed at discrete locations produces the following dispersion relation [10]:

$$\cos\left(\frac{L\Omega}{v} \pm \frac{L\omega_c}{2v}\right) = \cos\frac{L\omega_c}{2v} + \frac{\Gamma L}{\omega_c v}\sin\frac{L\omega_c}{2v} \qquad (2)$$

The discrete cavity dispersion relation of Eq. (2) yields a prediction of 24 dB growth in the BBU, when the effect of frequency spread is taken into account, i.e. the growth in each cavity is summed using the individual parameters for each cavity (See Table 1).

An unfortunate circumstance in this experiment is the fact that in order to increase the amount of transported current, the applied magnetic field must also be increased. Therefore, it is difficult to determine the scaling of the BBU growth versus current while holding the magnitude of the focusing field constant or vice versa. An attempt to incorporate the I vs. B dependence into the growth rate analysis examines the BBU growth rate versus the ratio of current to magnetic field, I/B. Figure 4 plots the experimental and theoretical growth of the BBU versus I/B using the two-dimensional continuum theory, Eq. (1).

In Figure 4, it is evident that the BBU growth predicted by continuum theory (open squares) agrees well with BBU growth in experiments with low I/B. For large values of I/B,

however, there is significant divergence between theory and experiment. Application of the discrete cavity theory, Eq. (2), does not provide much better agreement. An explanation for this difference between theory and observation could be "beam loading", which changes the electromagnetic properties of a cavity by the presence of an e-beam. One effect of beam loading is to shift the resonant frequency according to [11]

$$\omega_o' = \sqrt{\omega_o^2 + \omega_{pe}^2} \qquad (3)$$

where ω_o' is the corrected upshifted resonant frequency, ω_o is the angular resonant frequency of the cold cavity, and ω_{pe} is the angular plasma frequency of the electron beam given by

$$\omega_{pe}^2 = \frac{4 I_b c^2}{r_w^2 (17\ \text{kA})} \sqrt{\frac{1+\alpha^2}{\gamma^2 - 1}} \quad , \qquad (4)$$

where I_b is the beam current, r_w is the radius of the beam, and α is the perpendicular to parallel electron velocity ratio. For example, an electron beam with parameters: I_b = 100 A, V = 750 kV, r_w = 6.9 cm, and α = 0.1, and $\omega_o = 2\pi \times 2.523$ GHz, the corrected angular resonant frequency is $\omega_o' = 2\pi \times 2.524$ GHz. This increase may seem slight but it is important to remember that the cavities have a high Q (narrow line width). For I_b = 128 A the resonance of the average cavity is shifted 0.05 %. This shift is equal to the line width of a cavity with Q = 1000.

In other words, if the current is high enough then the beam can "detune" the cavities with respect to the beam modulation-cavity resonance condition which drives the BBU. The effect of this shift is that the frequency of the BBU disturbance (equal to the priming frequency) is too low to drive the (detuned) TM_{110} mode, leading to the observed reduction of BBU growth in the experiments.

Figure 5 shows the difference between the predicted magnitude of BBU growth from continuum theory and the observed growth ($\Gamma_{theory} - \Gamma_{experiment}$) versus transported current. It is interesting to note that significant difference appears to begin at approximately 100 A, which is where the frequency upshift begins to become equivalent to the line width of the average cavity.

In order to gain further understanding of the detuning phenomenon and its effect on the BBU growth rate, experiments in which the priming frequency was changed were carried out.

These experiments could be considered as the converse of beam loading. In beam loading, the resonant frequencies of the cavities are detuned with respect to the frequency of the beam modulation. Changing the priming frequency, however, causes the beam modulation to be altered with respect to the cavity resonant frequencies. For these experiments the beam current is kept low (< 50 A) so that the beam loading effect is slight. An advantage in this case is that the priming frequency can be very accurately determined, whereas detuning through beam loading is ambiguous because of uncertainties in the exact frequency upshift, and differences in Q's and variations in resonant frequencies among the cavities.

When the priming microwaves are turned off, very little signal is observed on the crystal detectors, indicating undetectable instability growth arising from noise over the ten cavities. This suggests that the frequency of modulation applied to the beam through priming will be the dominant frequency available for BBU growth. In other words, the effect of priming is so strong that any growth at any other frequency will be small compared to the BBU growth of the priming microwaves. This feature has the additional advantage of observing BBU growth at a frequency other than the exact resonant frequency.

A summary microwave growth for several shots taken over a range of priming frequencies is shown in Figure 6. The currents for these data range from 40 to 50 A and the applied magnetic field for all shots is 1.1 kG . Superimposed on the data are the dispersion relations, Im(k), from the continuum theory Eq. (1) (thin lined curve), and the discrete cavity theory, Eq. (2) (thick lined curve), with ω equal to the priming frequency. The continuum theory uses ω_o equal to the average cavity TM_{110} resonant frequency of 2.523 GHz and thus neglects frequency spread. The discrete cavity theory is the sum of predicted growths resulting from each cavity using each cavity's own ω_o and Q. The peaking of the data near the average TM_{110} resonant frequency is evidence that the beam breakup instability is indeed responsible for the observed microwave growth. The data also trace a broader curve than the continuum theory. This feature is due to the resonant frequency spread among the cavities in the array. The initial cavity's TM_{110} resonant frequency is 2.519 GHz. Thus, the TM_{110} fields are strongest and produce the most initial beam

modulation when the priming is tuned to 2.519 GHz. When the priming frequency is between 2.519 and 2.523 GHz the initial modulation is less, but the BBU has a higher growth rate as the frequency of the instability nears the average resonant frequency. Thus, the total amplitude of microwave growth is about the same in this region. Beyond 2.523 GHz the microwave growth diminishes rapidly following the theoretical curves.

The detuning experiments show that the coupling between the beam modulation and cavity fields is strongly dependent upon the resonant condition. A goal of this experimental program was to discover the experimental growth rates over a large range of currents and magnetic fields, and compare these rates to theory. The theory has proven accurate at low currents, but at high currents the experiment has not given the existing theory a fair chance, because of beam loading and the significant spread in the resonant frequencies. Some obvious improvements to this situation are apparent. One improvement would be to accurately match (« 0.1 %) the TM_{110} resonant frequencies. Especially important would be to match the frequency of the initial priming cavity to the average resonant frequency. A solution that accomplishes this was to lower the Q's of the cavities, the result of which is reported next.

III. LOW Q, SMALL FREQUENCY SPREAD EXPERIMENTS

In an attempt to create a fair test between theory and experiment that would be valid at high e-beam currents, the cavity array was modified to a lower average Q, and a lower frequency spread. Table 2 lists the TM_{110} mode parameters for this second array. The Q lowering was achieved by inserting a thin annulus of microwave absorber (Eccosorb) into each cavity.

The BBU growth results from this set of ten cavities has been published elsewhere (see Ref. 3), but they are included on the right hand side of Figure 7. Note that there is no significant deviation from theoretical growth at high values of I/B.

Experiments using an additional nine cavities, for a total of 19, have been recently performed. The experimental arrangement schematic is shown in Figure 8. A longer (2 m)

solenoidal drift tube was employed, but otherwise the configuration and diagnostics are similar to those of the ten cavity experiments (shown in Figure 2). The parameters for the additional nine cavities (#11 - #19) are shown in Table 3.

The left portion of Figure 7 illustrates the BBU growth versus I/B for the nineteen cavity system. The lower I/B values for the nineteen cavity experiment are due to the lower magnetic field and thus lower transported current capable of being generated by the 2 m solenoid. For each experimental datum the corresponding discrete-cavity theoretical growth is also plotted. Note that the slope of the growth for the 10 cavity case is approximately half of that for the 19 cavity case, as expected.

Experimental data was also taken to gain information about the dispersion relation when $\omega \neq \omega_0$ for the ten cavity case and is shown in Figure 9. Just as in the high Q, large frequency spread experiments, the priming frequency was tuned off resonance to see how it affected the growth rate. This set of experiments was also presented in Ref. 3, but is reproduced here for a ready comparison with Figure 6. The plotted points (filled circles) are experimental data taken at the same magnetic field (3.4 kG) and nearly the same e-beam current (190-215 A). The thick lined curve is the BBU growth as predicted by the discrete-cavity equation (2) using I=210 A, and using each cavity's specific resonant frequency and Q. The thin lined curve is the continuum BBU growth equation (1) for the same parameters, but uses the average ω_0 of $2\pi \times 2.5075$ GHz and the average Q of 215. Note that the data follow the discrete cavity theory more closely in this case as well.

IV. BBU REDUCTION USING EXTERNAL CAVITY COUPLING

A. Experimental Results

The purpose of the experimental program described in this paper is two-fold. The first objective of this research was to successfully describe the behavior of the beam breakup instability by building an experiment specifically designed to study the BBU growth in a controlled manner. The results of the 10 cavity low Q, small frequency spread experiments detailed above and in Ref.

3 provide a good basis for pursuit of the next goal. The second intent of these experiments is to develop novel techniques for suppression of the BBU. In the high Q, large frequency spread case, BBU was reduced by beam loading and inadvertent stagger tuning. The knowledge that these effects can reduce BBU growth rates is not particularly novel. The use of RF cures of these types have been studied elsewhere [2,9,12-14], although it was beneficial to confirm BBU growth reduction through these mechanisms.

A notably novel mechanism for BBU reduction has been suggested theoretically by Colombant, Lau, and Chernin[15] and is particularly capable of being tested by the MELBA experiments. This method has been termed "external cavity coupling" and the initial experimental results using this method are detailed in Ref. 4. In this method the main beam cavities are coupled by transmission line to identical external dummy cavities on the outside of the transport structure. The idea here is that the beam cavities are capable of "sharing" deflecting mode energy with the dummy cavities and thus reduce the magnitude of the TM_{110} mode fields in the beam cavities, with subsequent reduction in the BBU growth rate [16,17]. The ten cavity MELBA experimental configuration is readily adaptable to this method, since each cavity contains a coupling loop antenna to sample the TM_{110} microwaves. Each antenna can be connected to a coaxial cable to transmit the microwaves out of the cavity. In this way, the loop antennas can double as a microwave sampler and as a device to deliver the TM_{110} mode energy to a dummy cavity containing a similar coupling loop.

Figure 10 shows the experimental configuration used for the external cavity coupling experiments. This arrangement is almost identical to the configuration used for the low Q, small frequency spread baseline growth experiments described in Section III. The difference is that the seven intermediate cavities (#3 through #9) between the second and tenth have their coupling loops connected via microwave cable to seven nearly identical cavities located externally to the solenoid drift tube. The length of this cable was chosen to be 16 wavelengths long. Typically an experimental run alternated between a few shots with the internal and external cavities coupled (loop antennas connected) followed by a few shots with the internal and external cavities

uncoupled. When the cavities are uncoupled, the experiment is equivalent to the baseline low Q, large frequency spread BBU growth experiments described above.

A summary of BBU microwave growth data from some forty shots (from Ref. 4) is presented in Figure 11. The data show a consistent reduction of BBU growth from an average of 36 dB ($\sigma = \pm$ 1.5 dB) for the uncoupled case to an average of 30 dB ($\sigma = \pm$ 2.4 dB) for the coupled-cavity case. Thus, an average reduction in the BBU of 6 dB is measured for this system in which seven internal beam cavities are coupled to a nearly identical set of seven external dummy cavities[4].

B. Coupling Constant, κ, Determination

Previous analysis [4] has shown that the BBU spatial growth rate, Γ (where total BBU growth is given by $e^{\Gamma z}$), is modified by a factor of $1/(1+\kappa^2Q^2)$ to account for cavity coupling though a mutual inductance model [15-17]. Thus, the external coupled cavity growth rate is $\Gamma/(1+\kappa^2Q^2)$. Here, κ is the coupling constant and Q is the cavity quality . This factor of κ^2Q^2 represents the ratio of power leaked to the dummy (external) cavity to the power remaining in the main (internal) cavity [4]. A cold test was performed on a network analyzer (HP-8510) using two model cavities each with two coupling antennas. One antenna in each cavity was used to inject the microwaves and the second was used to transmit the RF power out of the cavity. This cold test experiment indicated that the power sharing ratio for this arrangement is $\kappa^2Q^2 = 0.13$. Using this value in the reduction factor yields an expected experimental reduction to 36 dB(1/1.13) ≈ 32 dB.

However, the cold test of the power sharing ratio differs from the actual experimental configuration. In the experiment, each cavity has only one coupling loop, thus the cold test may underestimate the magnitude of power sharing since the extra antennas provide additional inductance to the overall circuit. An alternative method to determine κ has been developed using an equivalent circuit model similar to those used in coupled cavity klystron analyses[18]. The equivalent circuit representing the experimental configuration is shown in Figure 12. The critical parameter that governs the magnitude of power sharing is the mutual inductance, M, connecting the

loop antenna circuits to the cavity circuits. The mutual inductance can be found from the formula[19,20]:

$$\frac{\omega_o^2 M^2}{R} = \frac{2s^2 J_1^2\left(\frac{3.83\,r}{b}\right) Q}{J_o^2(3.83)\varepsilon_o r^2 \pi b^2 \ell Z_o \omega_o}, \qquad (5)$$

where ω_o is the angular TM_{110} resonant frequency, R is the resistance assigned to the cavity circuit, s is the area of the coupling loop, r is the radial position of the antenna in the cavity, b is the radius of the cavity, ℓ is the cavity length, and Z_o is the characteristic impedance of the coupling cable. Table 4 lists the circuit parameters shown in Figure 12. Solving for power in the main and dummy cavities with the circuit program SPICE [21] yields a power sharing ratio of $\kappa^2 Q^2 = 0.18$. Use of this value in the $1/(1+\kappa^2 Q^2)$ reduction factor gives a predicted value of 30 dB growth for the coupled cavity experiments. This results in better agreement between theory and experiment than that reported in Ref. 4.

It might be argued that cavity coupling is equivalent to the often used BBU reduction technique of Q lowering, because both methods serve to lower the strength of the TM_{110} mode fields. There is a significant difference, however. A finite Q represents lossy processes from which energy cannot be recovered, whereas a nonzero κ represents only reactive loading which does not result in any energy loss. If Q were set to infinity, i.e. no dissipative losses, the process of power sharing would still exist and BBU growth rate reduction would still occur [15]. Therefore, this technique provides a novel way in which to reduce the adverse effects of the beam breakup instability.

V. CONCLUSIONS

This paper contains the results of an experimental program whose only goal is to investigate the behavior of the beam breakup instability. Through the course of this research

several original developments have been made regarding the physics of the beam breakup instability. These developments come in the form of advancements in the applied theory of BBU, such as the validation of the continuum model in a few (10) cavity system, experimental investigations of untested theoretical regimes, and demonstration of a novel BBU growth reduction technique.

ACKNOWLEDGMENTS

This research was supported by Strategic Defense Initiative Office of Innovative Science and Technology managed by the Office of Naval Research. Support for PRM also supplied by a Rackham School of Graduate Studies Fellowship.

REFERENCES

1. W. K. H. Panofsky and M. Bander, Rev. Sci. Instrum. 39 (2), 206 (1968).
2. R. Helm and G. Loew, Beam Breakup, Chapter B.1.4 in *Linear Accelerators*, P.M. Lapostelle and A.L. Septier, Editors, p. 173 (North Holland Publishing Co., Amsterdam, 1970).
3. P.R. Menge, R.M. Gilgenbach, and R.A. Bosch, Appl. Phys. Lett. 61 (6), 642 (1992).
4. P.R. Menge, R.M. Gilgenbach, and Y.Y. Lau, Phys. Rev. Lett. 69 (16), 2372 (1992).
5. V.K. Neil, L.S. Hall, and R.K. Cooper, Part. Accel. 9, 213 (1979).
6. G. J. Caporaso, F. Rainer, W. E. Martin, D. S. Prono, and A. G. Cole, Phys. Rev. Lett. 57 (13), 1591 (1986).
7. Y.Y. Lau, Phys. Rev. Lett. 63 (11), 1141 (1989).
8. V.K. Neil and R.K. Cooper, Part. Accel. 1, 111 (1970).
9. D. G. Colombant and Y. Y. Lau, Appl. Phys. Lett. 55 (1), 27 (1989).
10. R. A. Bosch, P.R. Menge, and R. M. Gilgenbach, J. Appl. Phys. 71 (7), 3091 (1992).
11. R.E. Shefer and G. Bekefi, Internat. J. Elect. 51 (4), 569 (1981).
12. R. L. Gluckstern, F. Neri, and R. K. Cooper, Part. Accel. 23, 37 (1988).
13. D. Chernin and A. Mondelli, Part. Accel. 24, 177 (1989).
14. K. A. Thompson and R. D. Ruth, Phys. Rev. D 41 (3), 964 (1990).
15. D. Colombant, Y. Y. Lau, and D. Chernin, Part. Accel. 35, 193 (1991).
16. D.G. Colombant and Y.Y. Lau, J. Appl. Phys. 72 (9), 3874 (1992).
17. D. Colombant and Y. Y. Lau, Nuc. Instrum. Meth. A311, 1 (1992).
18. R.E. Collin, *Foundations for Microwave Engineering* (McGraw-Hill, Singapore 1966), Chapter 9.
19. R.A. Bosch, P.R. Menge, and R.M. Gilgenbach, "Reduction of Beam Breakup Growth by Coupling to External Bleeding Cavities", unpublished (1991).
20. P.R. Menge, Ph. D. Dissertation, The University of Michigan, 1993.

21. P.W. Tuinenga, *SPICE, A Guide to Circuit Simulation and Analysis Using PSpice* (Prentice Hall, Englewood Cliffs, NJ, 1988).

Tables:

Table 1

Parameters For High Q, Large Frequency Spread Cavities.

Cavity #	TM_{110} Resonant Frequency (GHz)	TM_{110} Q
1	2.5190	660
2	2.5200	1090
3	2.5200	1420
4	2.5201	1800
5	2.5265	530
6	2.5270	680
7	2.5230	1160
8	2.5240	920
9	2.5248	680
10	2.5250	1010
average	2.5230 ± 0.1 %	1000 ± 310

Table 2

Parameters for Low Q, Small frequency Spread Cavities.

Cavity #	TM_{110} Resonant Frequency (GHz)	TM_{110} Q
1	2.5070	230
2	2.5070	290
3	2.5060	215
4	2.5082	220
5	2.5070	280
6	2.5072	230
7	2.5076	160
8	2.5078	185
9	2.5085	180
10	2.5086	170
average	2.5075 ± 0.03 %	215 ± 45

Table 3

Parameters For Additional Cavities In The 19 Cavity Experiment.

Cavity #	TM_{110} Resonant Frequency (GHz)	TM_{110} Q
11	2.5070	290
12	2.5079	250
13	2.5070	260
14	2.5073	300
15	2.5075	230
16	2.5076	190
17	2.5082	160
18	2.5085	300
19	2.5080	270
nineteen cavity average	2.5076 ± 0.03 %	230 ± 45

Table 4

Values of equivalent circuit components.

component	symbol	value
capacitance of cavities	C_m, C_d	29.6 fF
inductance of cavities	L_m, L_d	137 nH
resistance of cavities	R_m, R_d	10 Ω
inductance of coupling loop	L_ℓ	6.4 nH
resistance of coupling loop	R_ℓ	0.01 Ω
mutual inductance between loop and cavity	M	2.7 nH

Figure Captions:

Figure 1. Comparison of MELBA to other well-known accelerators in BBU growth rate parameter space (from Ref. 7).

Figure 2. Experimental configuration.

Figure 3. Experimental data taken from two similar shots: a) Diode voltage (310 kV/div), flattop is 750 kV. b) Injected current (92 A/div), maximum is 230 A. c) Transported current (40 A/div), flattop is 46 A. d) Detector signal of 2nd cavity RF (100mV/div), signal attenuated by 12 dB. e) Detector signal of 10th cavity RF (100mV/div), signal attenuated by 32 dB. Time scale is 100 ns/div. Solenoidal magnetic field is 1.1 kG.

Figure 4. Graph of beam breakup instability growth versus the ratio of transported current to magnetic field, I/B. For each point representing experimentally measured growth (black circles), the corresponding theoretical prediction for growth using the same beam parameters is also plotted (open squares). The lines are guides for the eye.

Figure 5. Graph showing the difference between theoretically computed and experimentally observed BBU growth (i.e. $\Gamma_{theory} - \Gamma_{experiment}$) versus transported beam current. Horizontal line shows position of exact agreement.

Figure 6. Microwave growth versus priming frequency. Experimentally observed microwave growth (black circles) is shown with the theoretical growth curves for I_b = 45 A and B = 1.1 kG. The thick lined curve is the predicted growth from the discrete cavity theory [Eq. (2)], and the thin lined curve uses the continuum theory which does not include frequency spread. The black triangles along the abscissa represent experimental growth below the level of detectability.

Figure 7. BBU growth (dB) versus ratio of beam current to magnetic field, I/B (A/kG). Experimental data (filled symbols) are plotted with corresponding theoretical growth (open symbols). Two experimental cases are shown: 19 cavities (squares) and 10 cavities (circles).

Figure 8. Nineteen cavity experimental configuration.

Figure 9. Microwave growth dependence on the frequency of priming microwaves. Experimental data are represented by the filled circles. The thicker curve is the theoretical growth predicted by the discrete-cavity theory. The thinner curve is the theoretical growth predicted by the continuum theory. The triangles along the abscissa indicate experimental growth below the level of detectability (from Ref. 3).

Figure 10. External coupled cavity configuration.

Figure 11. Growth (dB) of the BBU microwave power for forty different electron beam pulses showing uncoupled shots (open circles) and externally coupled shots (black squares) (from Ref. 4).

Figure 12. Equivalent circuit representing the coupled cavities in the actual experimental configuration.

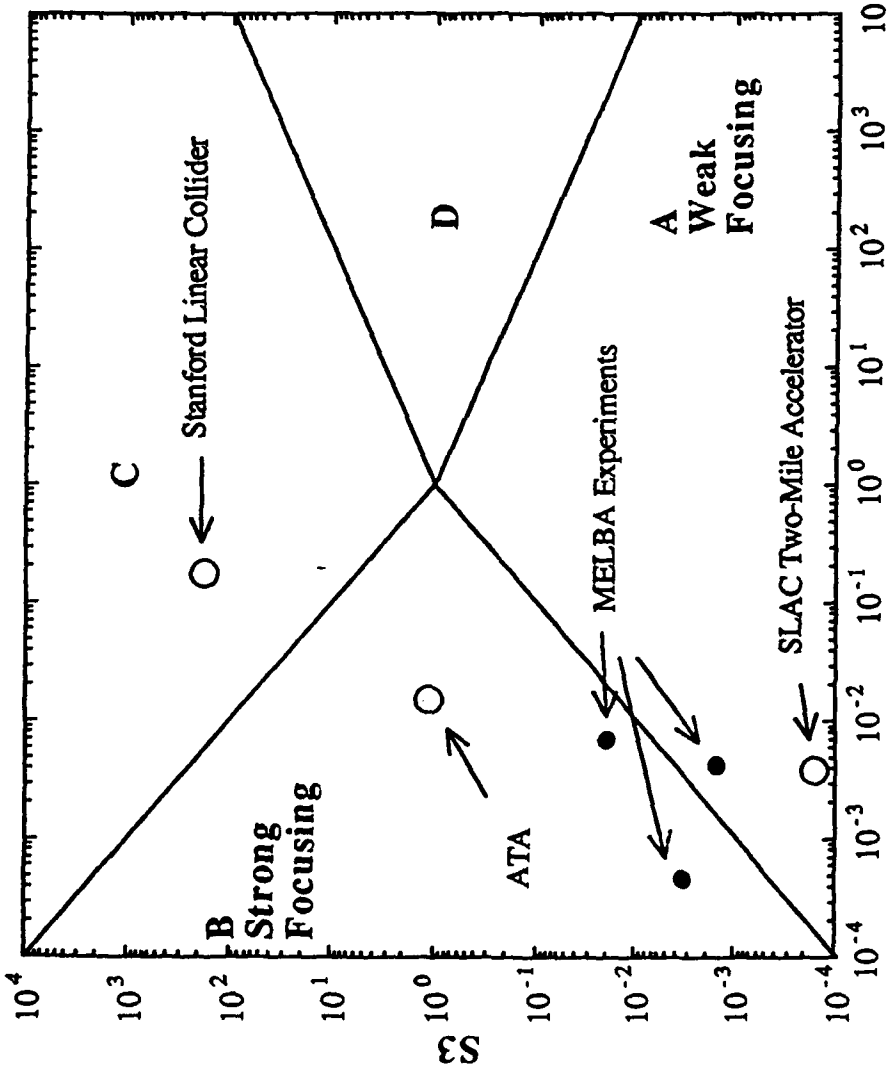
C
Stanford Linear Collider
D
A
Weak
Focusing
B
Strong
Focusing
ATA
MELBA Experiments
SLAC Two-Mile Accelerator
ε_3
ε_1
10^{4}
10^{3}
10^{2}
10^{1}
10^{0}
10^{-1}
10^{-2}
10^{-3}
10^{-4}

Fig. 1

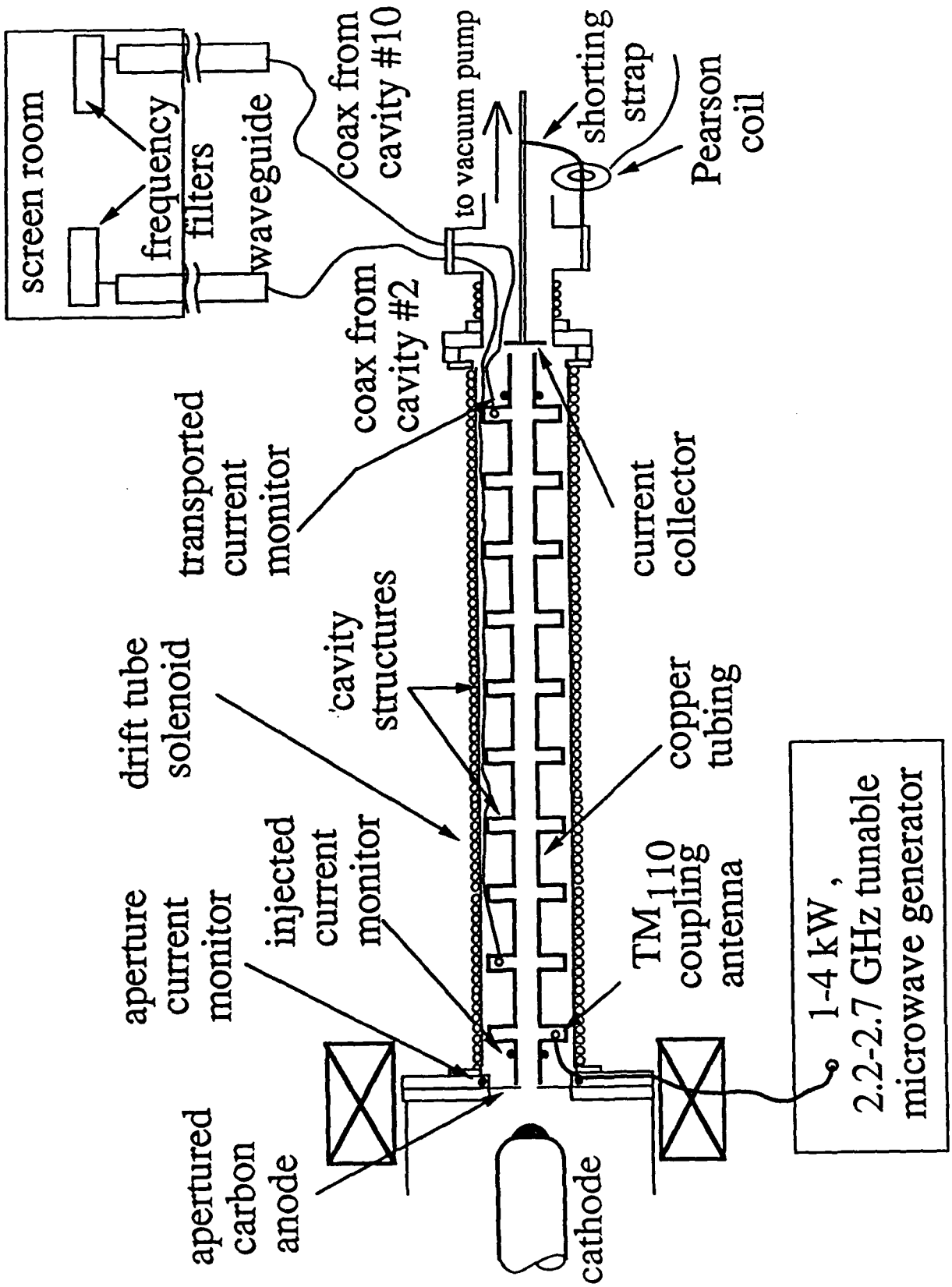
screen room
frequency
filters
waveguide
coax from cavity #10
to vacuum pump
shorting strap
Pearson coil
coax from cavity #2
transported current monitor
current collector
drift tube solenoid
cavity structures
copper tubing
aperture current monitor
injected current monitor
TM110 coupling antenna
1-4 kW, 2.2-2.7 GHz tunable microwave generator
apertured carbon anode
cathode

Fig. 2

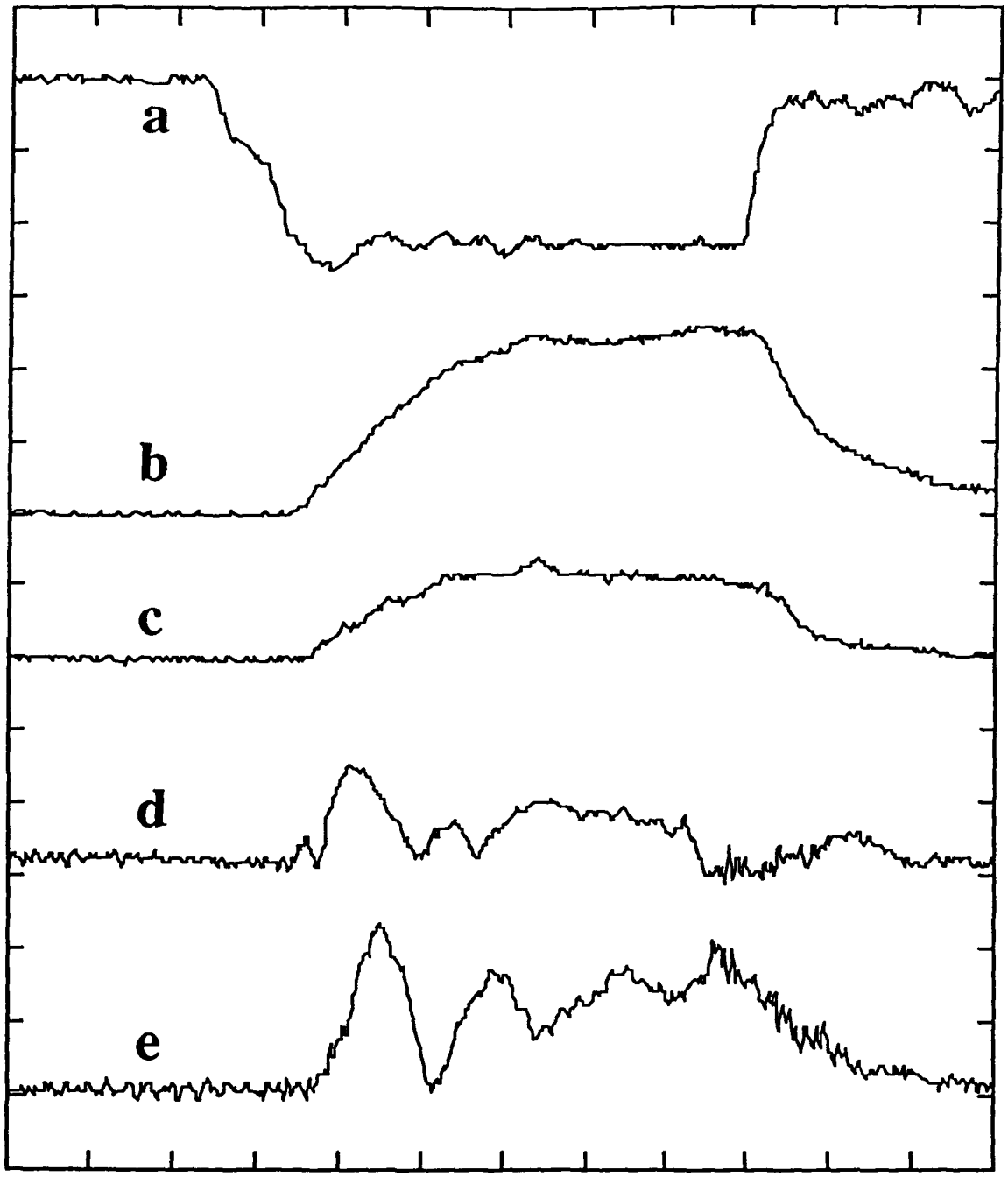

Figure 3

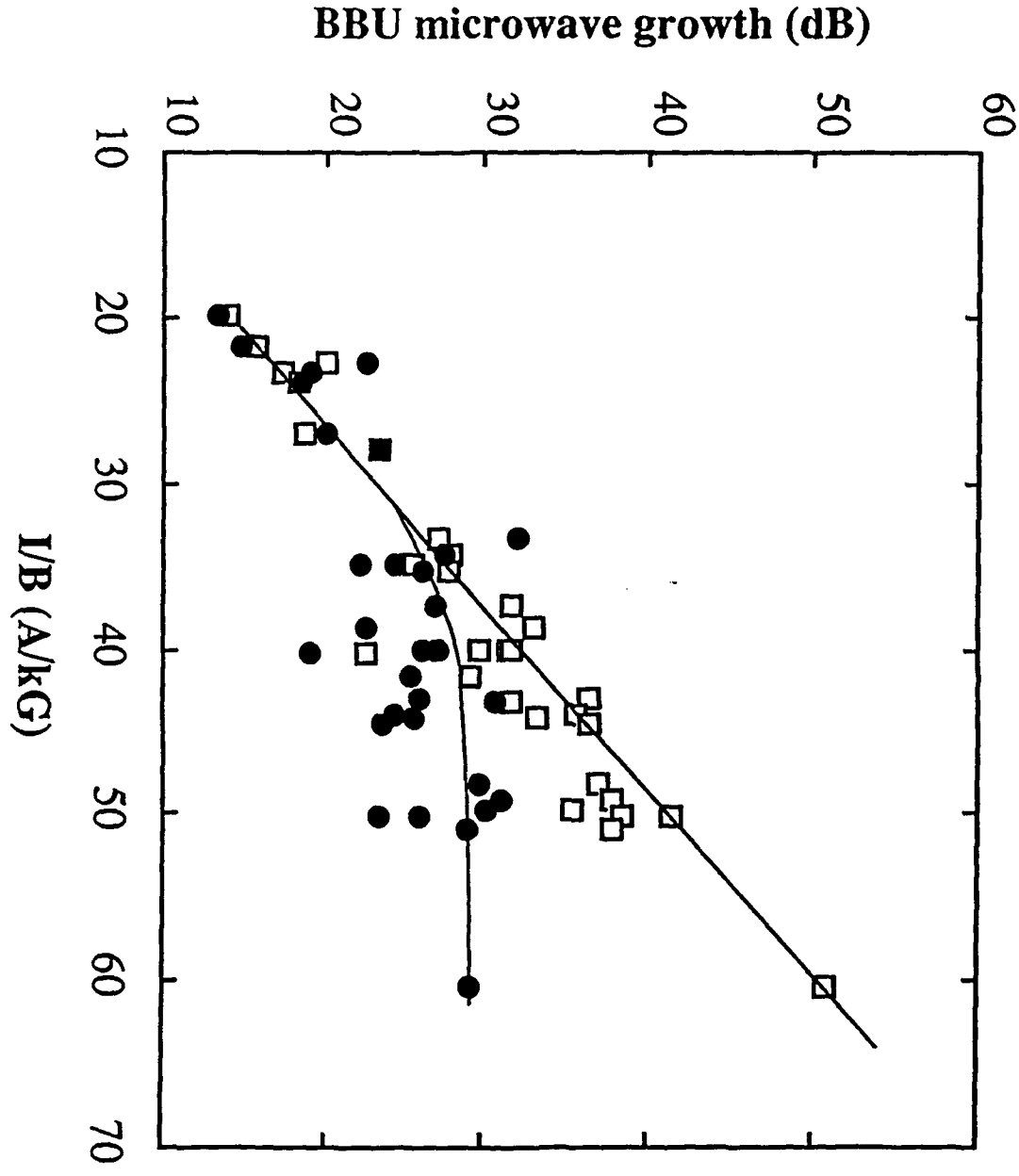
BBU microwave growth (dB)
10
20
30
40
50
60
I/B (A/kG)
10
20
30
40
50
60
70

Figure 4

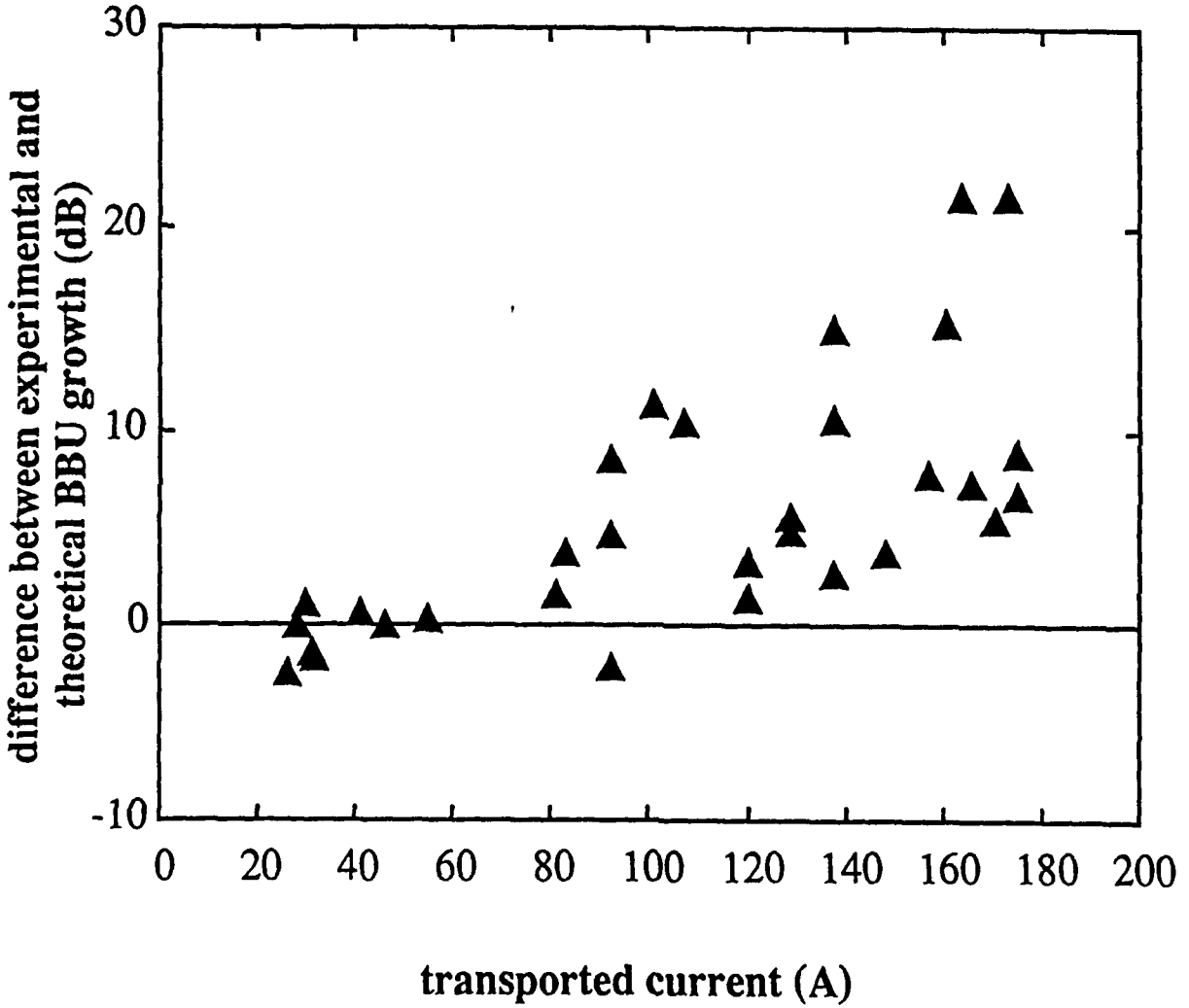
difference between experimental and theoretical BBU growth (dB)
30
20
10
0
-10
0
20
40
60
80
100
120
140
160
180
200
transported current (A)

Fig. 5

D 30

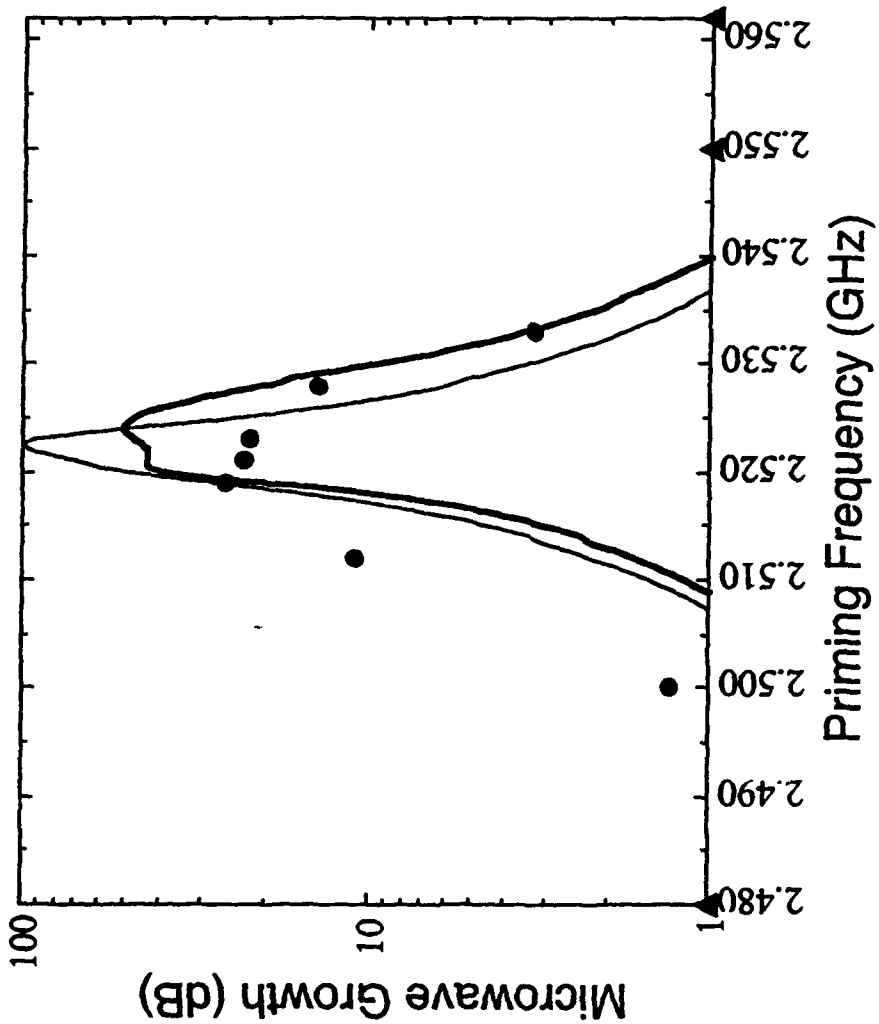
Microwave Growth (dB)
100
10
1
Priming Frequency (GHz)
2.480
2.490
2.500
2.510
2.520
2.530
2.540
2.550
2.560

Fig. 6

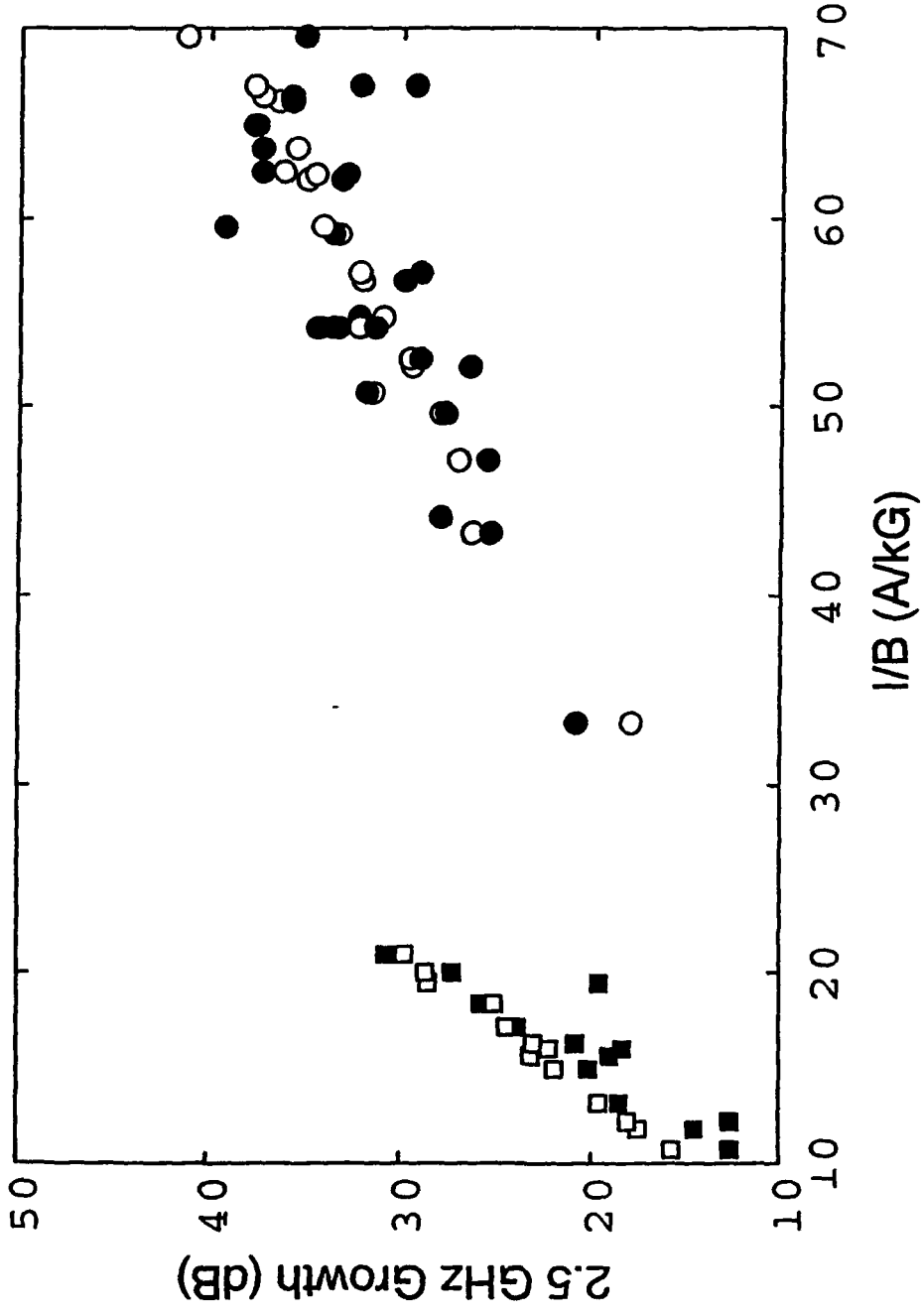

Fig. 7

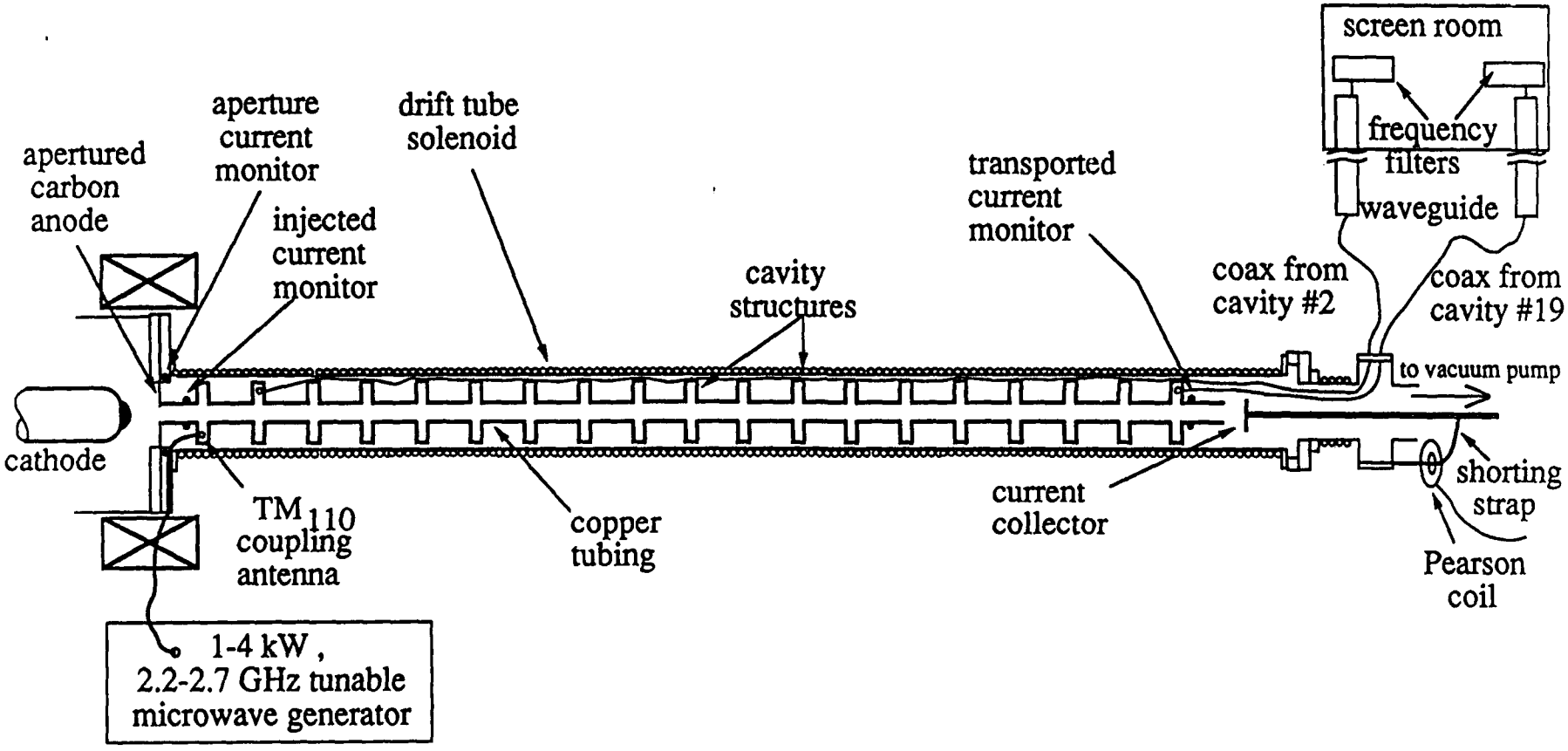
screen room
frequency
filters
waveguide
aperture
current
monitor
drift tube
solenoid
apertured
carbon
anode
injected
current
monitor
transported
current
monitor
cavity
structures
coax from
cavity #2
coax from
cavity #19
to vacuum pump
cathode
TM110
coupling
antenna
copper
tubing
current
collector
shorting
strap
Pearson
coil
1-4 kW ,
2.2-2.7 GHz tunable
microwave generator

Fig. 8

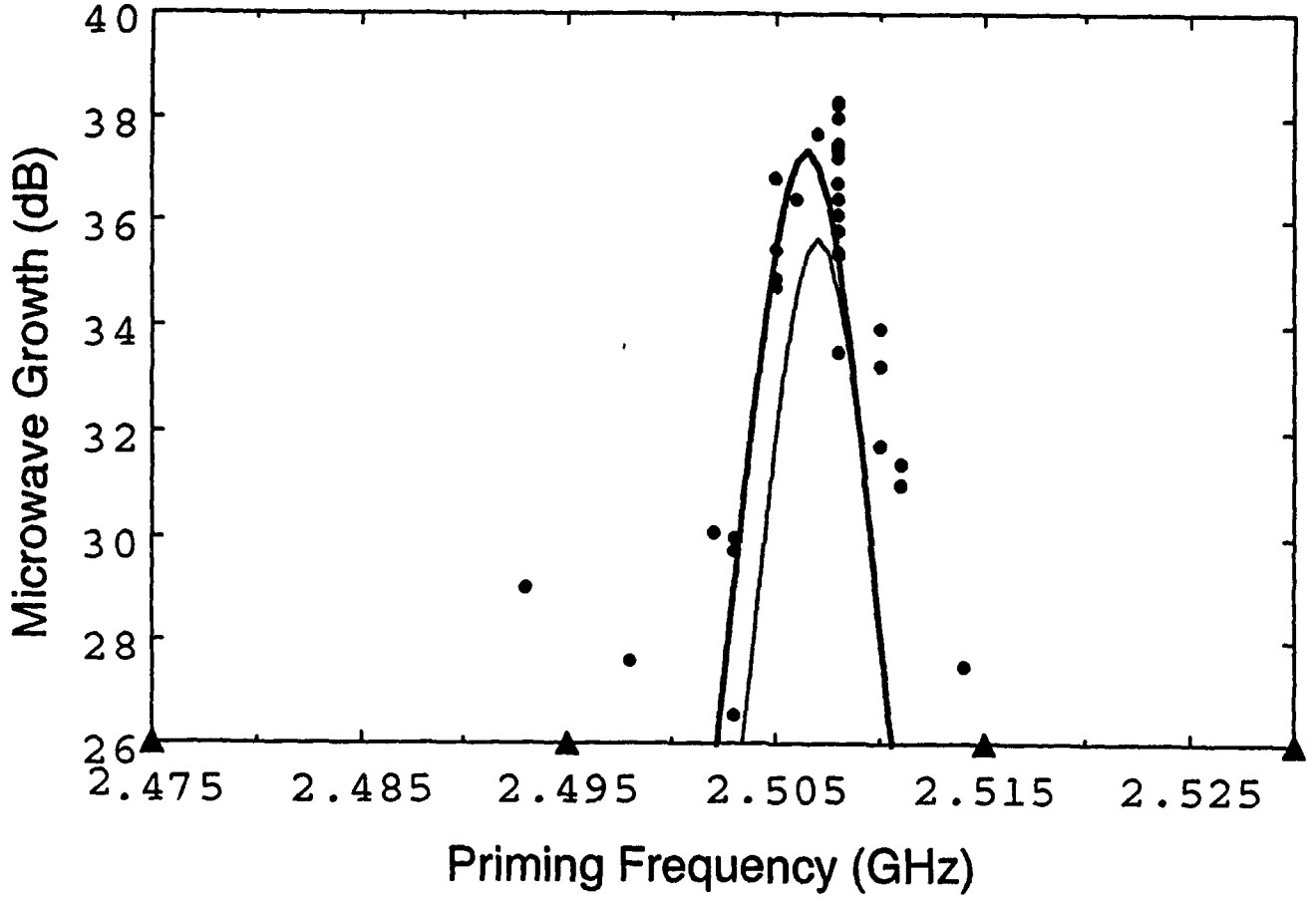
Microwave Growth (dB)
40
38
36
34
32
30
28
26
2.475
2.485
2.495
2.505
2.515
2.525
Priming Frequency (GHz)

Fig. 9

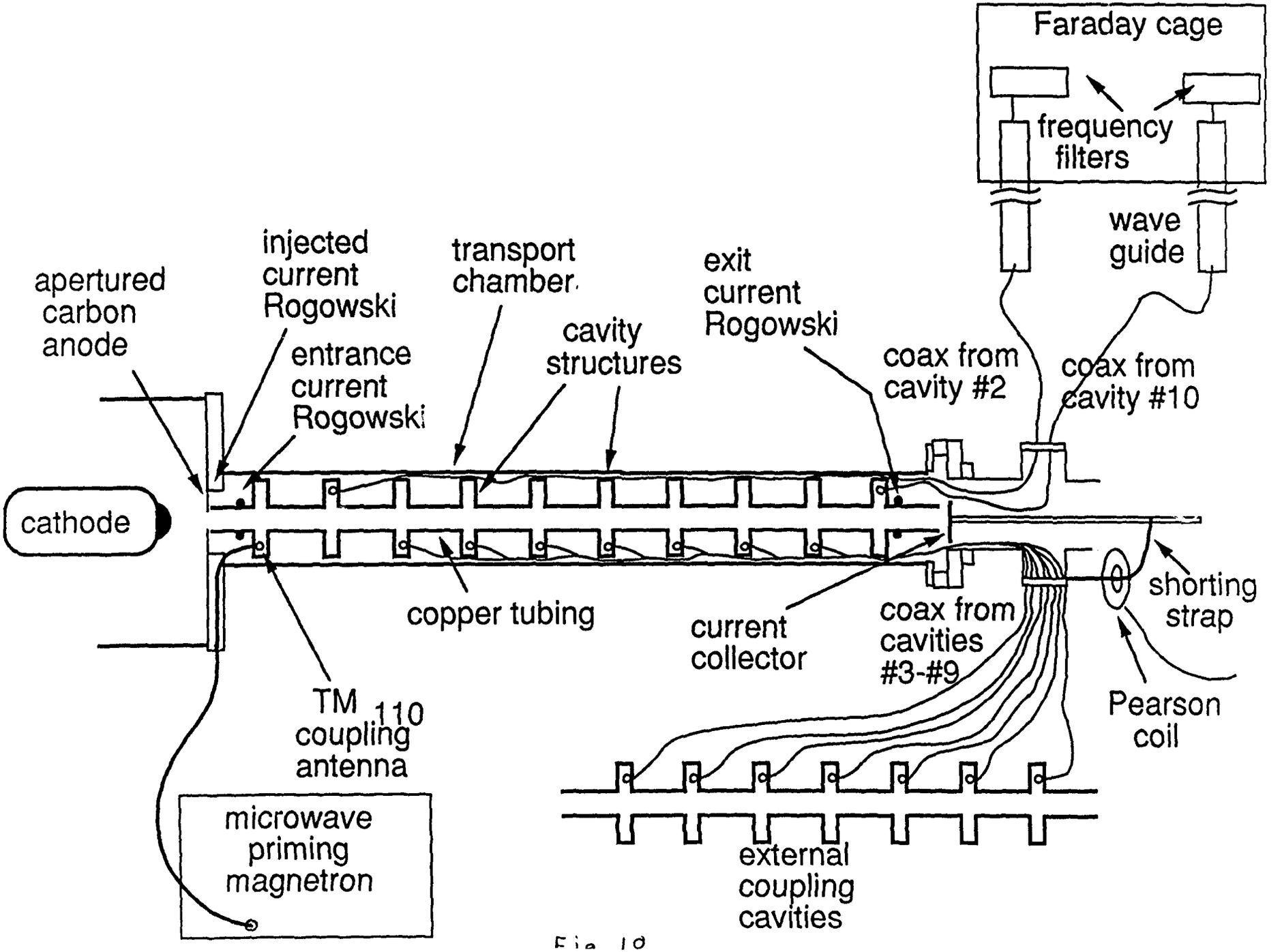
Faraday cage
frequency filters
wave guide
injected current Rogowski
transport chamber
exit current Rogowski
apertured carbon anode
entrance current Rogowski
cavity structures
coax from cavity #2
coax from cavity #10
cathode
copper tubing
current collector
coax from cavities #3-#9
shorting strap
Pearson coil
TM 110 coupling antenna
microwave priming magnetron
external coupling cavities

Fig. 10

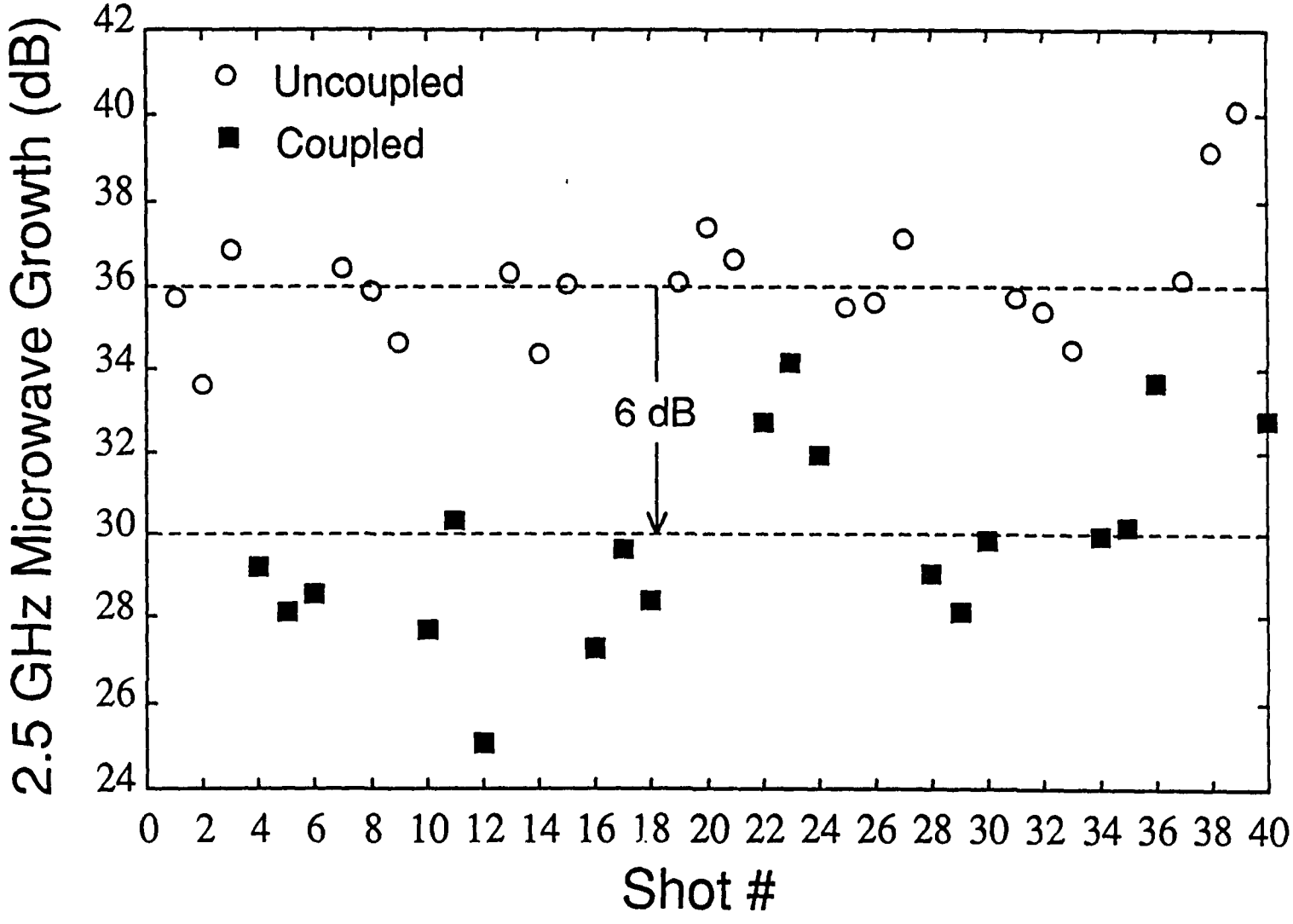
2.5 GHz Microwave Growth (dB)
42
40
38
36
34
32
30
28
26
24
Uncoupled
Coupled
6 dB
0 2 4 6 8 10 12 14 16 18 20 22 24 26 28 30 32 34 36 38 40
Shot #

Fig. 11

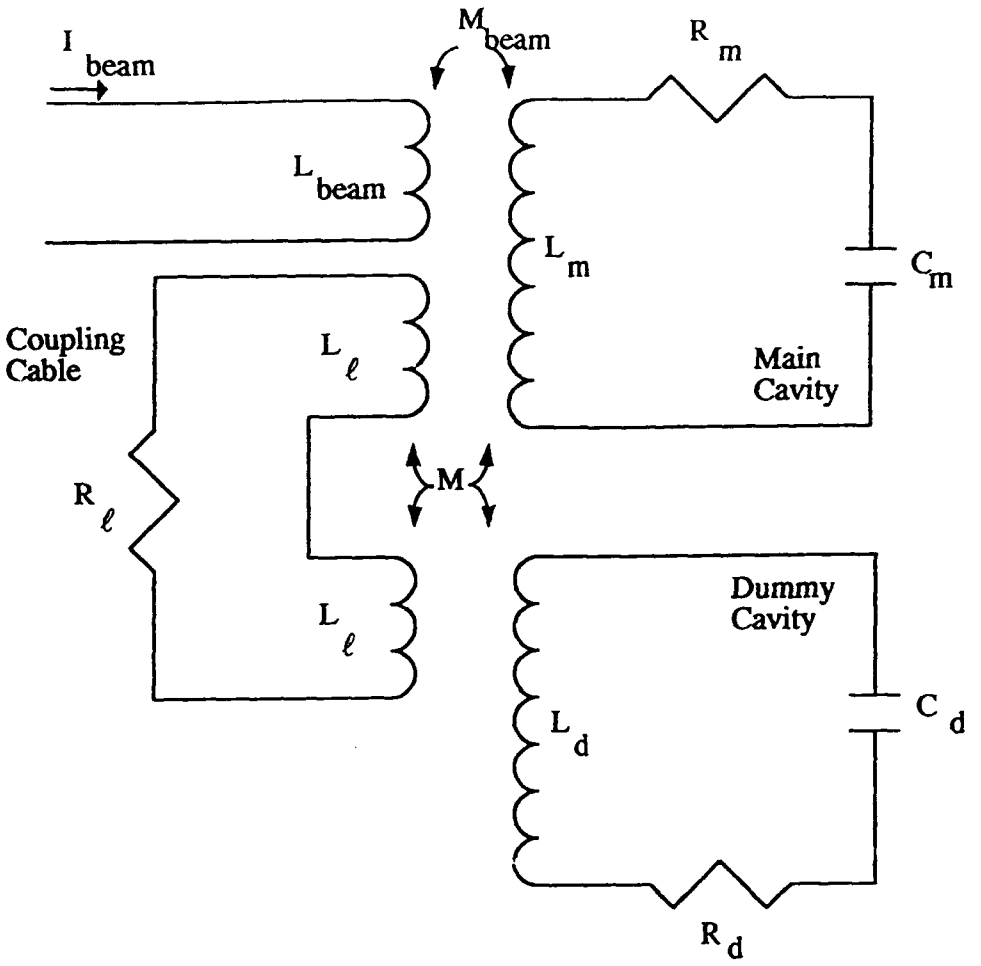
I beam
M beam
R m
L beam
L m
C m
Coupling Cable
L ℓ
Main Cavity
R ℓ
M
L ℓ
Dummy Cavity
C d
L d
R d

Fig 12